AWARD NUMBER: W81XWH-16-1-0474

TITLE: An Association of Unique microRNA Turnover Machinery with Prostate Cancer Progression

PRINCIPAL INVESTIGATOR: Hsieh, Jer-Tsong

CONTRACTING ORGANIZATION: University of Texas Southwestern Medical Center
Dallas, TX 75390

REPORT DATE: Oct 2019

TYPE OF REPORT: Annual

PREPARED FOR: U.S. Army Medical Research and Materiel Command

Fort Detrick, Maryland 21702-5012

REPORT DOCUMENTATION PAGE

Form Approved
OMB No. 0704-0188

1. REPORT DATE	2. REPORT TYPE	3. DATES COVERED
Oct 2019	Annual	09/15/2018-09/14/2019

4. Title

An Association of Unique microRNA Turnover Machinery with Prostate Cancer Progression

5a. CONTRACT NUMBER

5b. GRANT NUMBER
W81XWH-16-1-0474

5c. PROGRAM ELEMENT NUMBER

6. AUTHOR(S)
Jer-Tsong Hsieh

E-Mail: jt.hsieh@utsouthwestern.edu

5d. PROJECT NUMBER

5e. TASK NUMBER

5f. WORK UNIT NUMBER

7. PERFORMING ORGANIZATION NAME(S) AND ADDRESS(ES)

UT Southwestern Medical Center
5323 Harry Hines Blvd.,
Dallas, TX 75390

8. PERFORMING ORGANIZATION REPORT NUMBER

9. SPONSORING / MONITORING AGENCY NAME(S) AND ADDRESS(ES)

U.S. Army Medical Research and Materiel Command
Fort Detrick, Maryland 21702-5012

10. SPONSOR/MONITOR'S ACRONYM(S)

11. SPONSOR/MONITOR'S REPORT NUMBER(S)

12. DISTRIBUTION / AVAILABILITY STATEMENT

Approved for Public Release; Distribution Unlimited

13. SUPPLEMENTARY NOTES

14. ABSTRACT

Prostate cancer (PCa) is the second highest cancer mortality among male cancer in USA. This disease is still incurable because PCa once becomes metastatic and develops drug resistance when cancer cells undergo epithelial-to-mesenchymal transition (EMT) and acquire cancer stem cell (CSC) phenotypes. Emerging evidence has shown that the presence of metastatic PCa is associated with CSC phenotype that is likely associated with its resistance to radiation or chemotherapy. The preliminary data from this study clearly demonstrate that several tumor suppressor microRNAs (miRNAs) involved in regulating these processes are often degraded by IFIT5. Also, elevated IFIT5 is associated with PCa malignancy. Thus, this study will delineate the mechanism of IFIT5 in tumor suppressor miRNA degradation, and examine IFIT5 gene regulation. By determining its clinical correlation, this study will provide valuable biomarker(s) for lethality of PCa, which will an immediate impact on patient prognosis and selection for more suitable agent. The outcome of this study will provide a better understanding of miRNAs biogenesis associated with aggressive PCa exhibiting CSC phenotypes. Most importantly, the long-term the impact of this study will generate more effective therapeutic strategy of CRPC.

15. SUBJECT TERMS

16. SECURITY CLASSIFICATION OF:			17. LIMITATION OF ABSTRACT	18. NUMBER OF PAGES	19a. NAME OF RESPONSIBLE PERSON
a. REPORT	b. ABSTRACT	c. THIS PAGE			USAMRMC
Unclassified	Unclassified	Unclassified	Unclassified		19b. TELEPHONE NUMBER *(include area code)*

TABLE OF CONTENTS

1. INTRODUCTION

MicroRNAs (miRNAs) are small non-coding RNA molecules that regulate gene expression by post-transcriptional degradation or translational repressions by recognizing the 3'-UTR sequence of target mRNA from the specific seed sequence (ca. 2-7 nucleotides) of miRNAs (1). miRNAs have been shown to regulate approximate 60% protein-coding genes via post-transcriptional suppression by facilitating mRNA degradation, or translational inhibition. In general, miRNAs are initially transcribed into a long primary transcript by RNA polymerase II similar to cellular mRNA, and sequentially processed by Drosha and Dicer-mediated endonuclease cleavage to become mature miRNA (2-4). Nevertheless, miRNA biogenesis becomes more complicated when miRNAs are derived from the same gene cluster controlled by the same promoter and yet some is processed with different efficiency at the precursor or mature level (5, 6), which adds more complexities into the scheme of gene regulation.

Epithelial-to-mesenchymal transition (EMT) is considered an initial step for cancer cells to acquire the metastatic potentials. In prostate cancer, many studies have demonstrated the relationship of the onset of EMT phenotypes with cancer metastasis. Knowing EMT as a normal physiologic process takes place during embryonic development, therefore, the cancer cells undergoing EMT appear to have higher potential to acquire cancer stem cell (CSC) phenotypes (7). However, the molecular mechanism(s) associated with EMT or CSC in prostate cancer is not fully understood.

Our preliminary data clearly indicated that elevated IFIT5 is associated with malignant prostate cancer and IFIT5 can target many miRNAs with tumor suppressive function in preventing EMT and CSC, in which IFIT5 can be as a potential therapeutic target. Therefore, it is critical to dissect the mechanism of IFIT5 in degrading miRNA or the regulation of IFIT5. Also, significant clinical correlation of elevated IFIT5 expression in prostate cancer specimens prompt us to explore IFIT5 as prognostic marker for prostate cancer.

REFERENCES

1. Aalto AP, Pasquinelli AE. (2012) Small non-coding RNAs mount a silent revolution in gene expression. Curr Opin Cell Biol., 24:333-340.
2. Bartel DP. (2004) MicroRNAs: genomics, biogenesis, mechanism, and function. Cell, 116:281-297.
3. Feng Y, *et al*. (2011) Drosha processing controls the specificity and efficiency of global microRNA expression. Biochimica et Biophysica Acta, 1809:700-707.
4. Winter J, *et al*. (2009) Many roads to maturity: microRNA biogenesis pathways and their regulation. Nat. Cell Biol. 11:228-234.
5. Chaulk SG, *et al.* (2011) Role of pri-miRNA tertiary structure in miR-17~92 miRNA biogenesis. RNA Biol., 8:1105-1114.
6. Chakraborty S, *et al.* (2012) Pri-miR-17-92a transcript folds into a tertiary structure and autoregulates its processing. RNA, 18:1014-1028.
7. Garg M. (2015) Targeting microRNAs in epithelial-to-mesenchymal transition-induced cancer stem cells: therapeutic approaches in cancer. Expert Opin. Ther. Targets., 19:285-297.

2. KEYWORDS

Epithelial-to-mesenchymal transition, cancer stem cell, IFIT5, XRN1 microRNA, microRNA turn over.

3. ACCOMPLISHMENTS

Major goals and accomplishments

Aim 1 Dissect the mechanism of IFIT5-mediated miRNA turnover.

Major Task: Unveil new machinery of miRNA turnover**.**

Milestone: Manuscript on mechanism of miRNA turnover**.**

The manuscript has been published in Cancer Research this year.

Aim 2 Determine the regulation of IFIT5 gene in prostate cancer progression.

Major Task: Identify key regulator(s) and inducer(s) of IFIT5 gene expression**.**

Subtask 1: Determine the inhibitory mechanism of DAB2IP in regulating IFIT5 expression induced by IFN.

Completed with paper publication.

Subtask 2: Examine the mechanism of IFIT5 gene regulation in response to paracrine/juxtacrine stimulation.

Completed with paper publication.

Subtask 3: Determine the role of IFIT5 in prostate cancer progression

Previously, we have found IFIT5 can induce epithelia-to-mesenchymal transition (EMT) in prostate cancer leading to cancer metastasis. EMT is known as transdifferentiation that could undergo stem cell reprogramming. Thus, we hypothesized IFIT5 is involved in prostate cancer stem cell formation. From determining prostasphere formation (Figure1A), we observed the elevation of IFIT5 protein (Figure1B) as well as mRNA (Figure1C) in prostasphere from 4 different cell models. Indeed, the upregulation of IFIT5 mRNA is due to transcription activation (Figure 1D). Furthermore, manipulating IFIT5 levels by shRNA (Figure 1E) or cDNA overexpression (Figure 1E and F), the prostasphere formation can be reduced or increased respectively.

To determine the underlying mechanism, we can correlate three key stem cell regulatory genes (i.e., Lin 28, Nanog and Bmi1) with prostasphere (Figure 2). Knowing IFIT5-mediated tumor suppressor miRNA degradation, we searched potential targeted miRNA for these 3 genes and identified miR-101 and miR-128 as the key players. As shown in Figure 3, ectopic expression of miR-101 or miR-128 can reduce the prostasphere formation. Also, we have validated the targets of miR-101 or miR-128 as Lin 28, Nanog and Bmi1.

To confirm whether IFIT5-induced prostasphere formation can be mediated by IFNγ, we treated PCa cells with IFNγ for 48hrs and observed significant increases of prostasphere (Figure 4A and B) and decreased miR-101 and miR-128. (Figure 4C and

D). In addition, by knocking down either Lin28 or Bmi1, the number of prostatspher was significantly reduced (Figure 4C and). Taken together, these data demonstrate that IFNγ can induce prostate cancer stem phenotypes mediated by IFIT5-modulated miRNA turnover machinery.

Figure 1 The role of IFIT5 in cancer stem cell formation of prostasphere (A) PCa cell lines cultured under conventional adherent (Monolayer, M) or ultra-low attachment sphere-forming conditions (Sphere, S). (B-C) Induction of IFIT5 protein and mRNA level in spheres (S) derived from each PCa cell lines, compared to monolayer adherent culture (M). (D) Enhanced IFIT5 promoter activity in Du145 and LNCaP cell spheres. (E) The impact of IFIT5-shRNA knockdown (shIFIT5+) on sphere forming ability of Du145 cells, compared to control shRNA (shIFIT5 -). (F-G) The impact of IFIT5-overexpression (IFIT5) on sphere forming ability of 22Rv1 and LNCaP cells, compared to vector control (Vec).

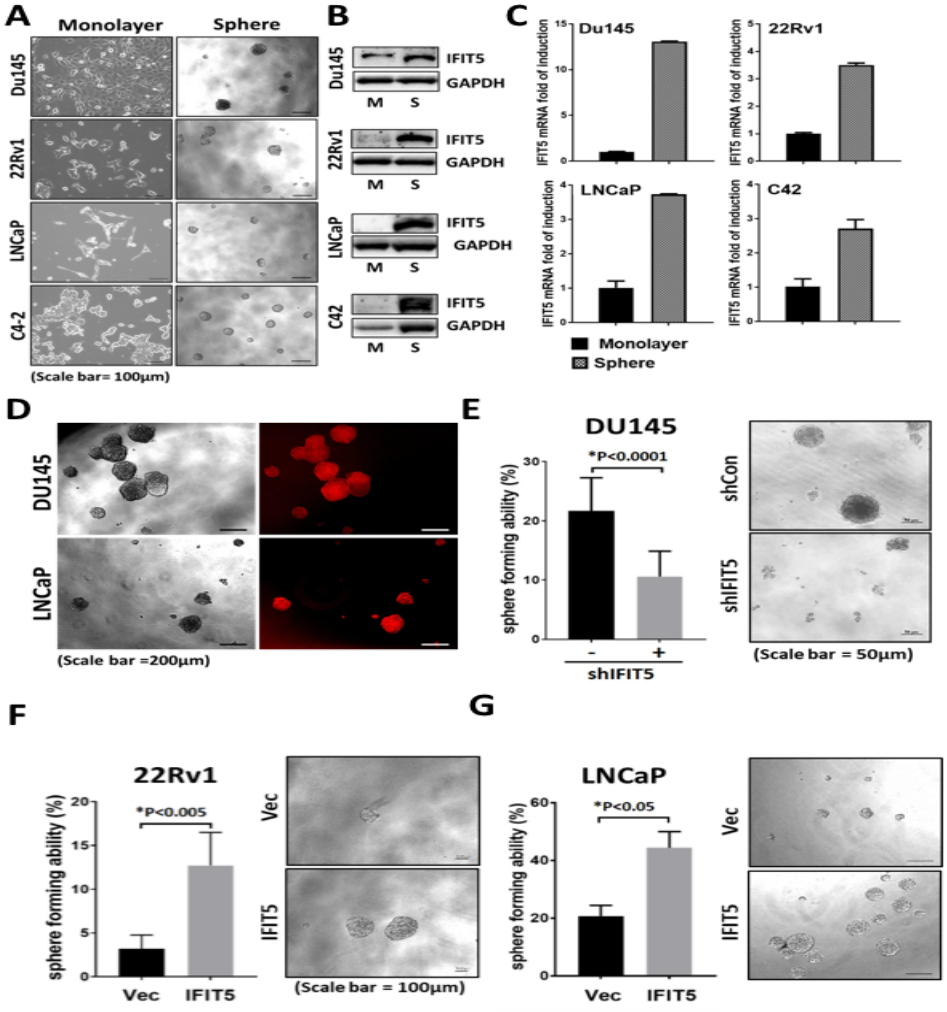

Figure 2 The association of Nanog, Lin28 and Bmi1 with prostate stem cell (A) Expression level of Nanog, Lin28, Bmi1 and IFIT5 mRNA in spheres derived PCa cell lines, compared to monolayer adherent culture. (B) Induced expression of Nanog, Lin28, Bmi1 and IFIT5 protein in spheres (S) derived PCa cell lines, compared to monolayer

adherent culture (M). (C) Expression of Nanog, Lin28, Bmi1 and IFIT5 mRNA and protein level in C4-2 spheres on day 5 and day 10 after seeding to the ultra-low attachment plate, compared to monolayer adherent culture. (D) Impact of IFIT5 on the mRNA expression level of Nanog, Lin28 and Bmi1 in PCa cell lines.

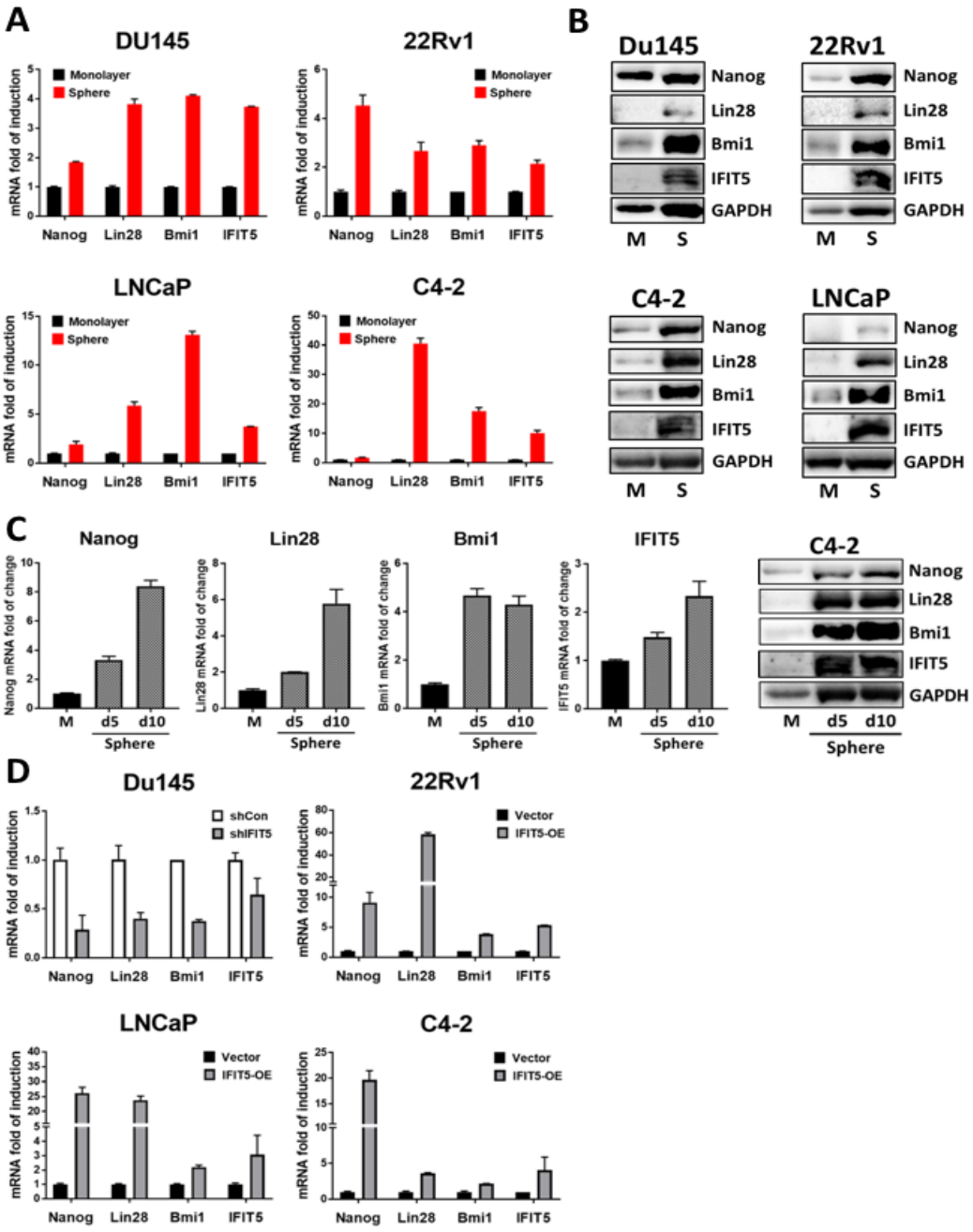

Figure 3 The suppressor effect of miR-101, -128 and -363 on prostasphere formation (A) Expression level of miR-101, miR-128 and miR-363 in spheres derived PCa cell lines, compared to monolayer adherent culture. (B) Overexpression of miR-128 and miR-101 in Du145 cells leads to differential suppression on the expression level of Lin28, Nanog and

Bmi1 mRNA. (C) The impact of miR-101 and miR-128 on the sphere forming ability of Du145, 22Rv1 and LNCaP cells.

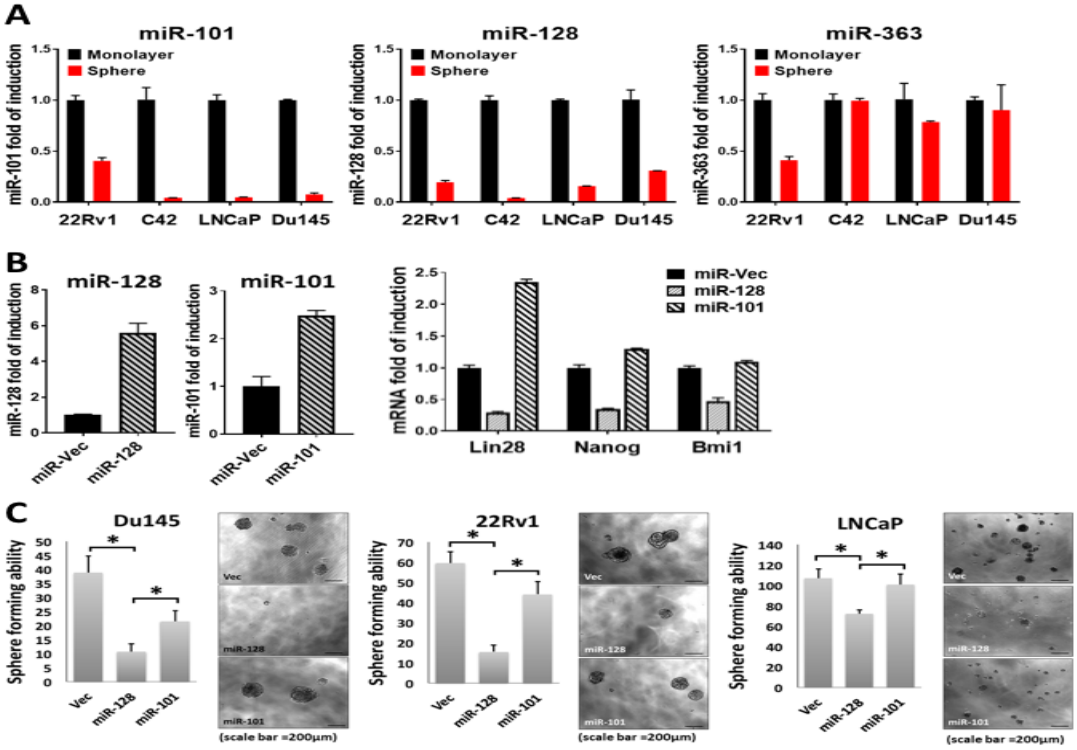

Figure 4 The induction of prostasphere by IFNγ (A-B) The impact of IFNγ on the sphere forming ability of Du145 and 22Rv1 cells. (C-D) The impact of native, DSMut- and SSMut-pre-miR-128 on the IFNγ-induced sphere formation of Du145 and 22Rv1 cells. (E) The impact of Lin28 shRNA knockdown on the sphere formation of Du145 cells (*P<0.05) (F) The impact of Bmi1 shRNA knockdown on the sphere formation of Du145 cells (*P<0.05)

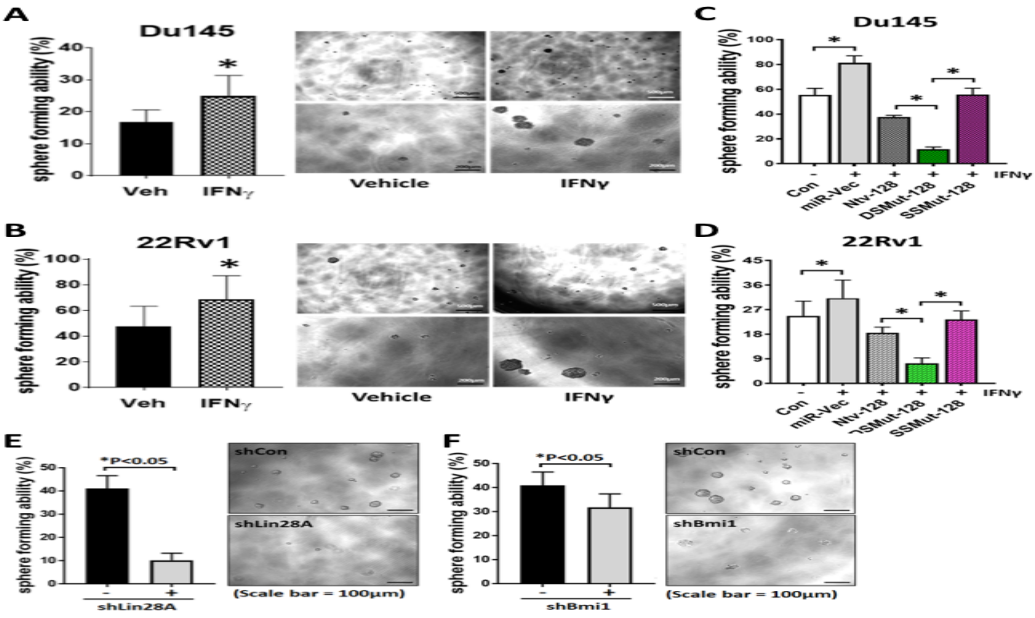

Aim 3 Evaluate IFIT5 as a prognostic marker in prostate cancer patients.

Major Task: Determine IFIT5 as a potential prognostic marker for prostate cancer.

Subtask 1: Collect clinical specimens and Study the clinical correlation of IFIT5 and miRNAs in prostate cancer progression.

In this aim, we proposed to collect clinical specimens for 30 months and determine IFIT5 mRNA and miRNA (-363, -101, and -128) levels in these specimens for clinical correlation. While we are still collecting patient specimens, we have decided to perform preliminary study to determine sample size. We have published these results in recent Cancer Research paper. In addition, we are making IFIT5 antibody in order to use immunohistochemical staining technique to validate gene expression results using different patient cohort.

Subtask 2: Examine the function of exosomal IFIT5 from patients
We have prepared exosome from several IFIT5-expressing culture cells and could not find the consistent results. Thus, we concluded that our previous finding may be due to the contamination of exosome preparation with death cells. Therefore, we focus on the cellular expression of IFIT5 in clinical specimens.

What opportunities for training and professional development have the project provided?
This project provides excellent training opportunities for molecular cell biology, tumor biology and pathohistologic techniques.

How were the results disseminated to communities of interest?
Currently, we have published three manuscripts. Also, we are preparing an abstract for submitting to AACR special conference of prostate cancer in 2019.

What do you plan to do during the next reporting period to accomplish the goals?
Currently, our progress is right on the target based on original SOW; we have completed Specific Aim 1 and the majority of Aim 2. Currently, one manuscript regarding the role of IFIT5 in cancer stem cell development is in the final preparation. In addition, we are testing antibody for IFIT5 in order to determine the correlation of IFIT5 with clinical manifestation of human prostate cancer.

4. IMPACT

What was the impact on the development of the principal discipline(s) of the project? What was the impact on other disciplines?
Our study unveils several tumorigenic roles of IFN in prostate cancer including induction of epithelia-to-mesenchymal transition and cancer stem cell. This study also demonstrates that several tumor suppressor microRNAs (miRNAs) involved in regulating these processes are often degraded by IFIT5. Also, elevated IFIT5 is associated with prostate cancer malignancy. Thus, this study will delineate the mechanism of IFIT5 in tumor suppressor miRNA degradation, and examine IFIT5 gene regulation. By determining its clinical correlation, this study will provide valuable

biomarker(s) for lethality of prostate cancer, which will an immediate impact on patient prognosis and selection for more suitable agent.
In addition, we have discovered a new function of IFIT5 complex as many tumor suppressor miRNA degradation machinery in prostate cancer. This discovery can certainly be applied onto other cancer types such as renal and liver cancers. In addition, the knowledge derived from this study can be used for designing better miRNA for therapeutic purpose.

What was the impact on technology transfer?
Nothing to Report.

What was the impact on society beyond science and technology?
Nothing to report.

5. CHANGES/PROBLEMS
Nothing to report.

6. PRODUCTS

Lo, U., Lee, C.F., Lee, M.S., Hsieh, J.T. (2017) The role and mechanism of epithelial-to-mesenchymal transition in prostate cancer progression. Int. J. Mol. Sci., 18: pii: E2079. PMID28973968

Lin CJ, Lo UG, Hsieh JT. (2018) The regulatory pathways leading to stem-like cells underlie prostate cancer progression. Asian J Androl. doi: 10.4103/aja.aja_72_18. PMID: 30178777

Lo, U., Pong, R.C., Yang, D., Gandee, L., Hernandez, E., Dang, A., Lin, C-J., Santoyo, J., Ma, S-H., Sonavane, R., Huang, J., Tseng, S-F., Moro, L., Arbini A.A., Kaour, P., Raj, G., He, D., Lai, C.H., Lin, H., Hsieh, J.T. (2019) Interferon-γ induces epithelial-to-mesenchymal transition in prostate cancer via a new mechanism of microRNA processing. Cancer Research, 79:1098-1112.

7. PARTICIPANTS AND OTHER COLLABORATING ORGANIZATIONS
Name: U-Ging Lo
Project Role: Research Scientist
No Change

Name: Payal Kapur
Project Role: collaborator
No Change

Has there been a change in the active other support of the PD/PI(s) or senior/key personnel since the last reporting period?
Nothing to Report.

What other organizations were involved as partners?

Nothing to Report.

8. SPECIAL REPORTING REQUIREMENTS

None.

9. APPENDIX

(1) Lo, U., Pong, R.C., Yang, D., Gandee, L., Hernandez, E., Dang, A., Lin, C-J., Santoyo, J., Ma, S-H., Sonavane, R., Huang, J., Tseng, S-F., Moro, L., Arbini, A.A, Kapur, P., Raj, G., He, D., Lai, C.H., Lin, H., Hsieh, J.T. (2019) IFN-γ-induced IFIT5 promotes epithelial-to-mesenchymal transition in prostate cancer via microRNAs processing. Cancer Res., 79:1098-1112. PMID30504123

Published OnlineFirst November 30, 2018; DOI: 10.1158/0008-5472.CAN-18-2207

Molecular Cell Biology

Cancer Research

IFNγ-Induced IFIT5 Promotes Epithelial-to-Mesenchymal Transition in Prostate Cancer via miRNA Processing

U-Ging Lo[1], Rey-Chen Pong[1], Diane Yang[1], Leah Gandee[1], Elizabeth Hernandez[1], Andrew Dang[1], Chung-Jung Lin[1], John Santoyo[1], Shihong Ma[1], Rajni Sonavane[1], Jun Huang[2], Shu-Fen Tseng[3], Loredana Moro[4], Arnaldo A. Arbini[5], Payal Kapur[6], Ganesh V. Raj[1], Dalin He[2], Chih-Ho Lai[7], Ho Lin[8], and Jer-Tsong Hsieh[1,9]

Abstract

IFNγ, a potent cytokine known to modulate tumor immunity and tumoricidal effects, is highly elevated in patients with prostate cancer after radiation. In this study, we demonstrate that IFNγ can induce epithelial-to-mesenchymal transition (EMT) in prostate cancer cells via the JAK–STAT signaling pathway, leading to the transcription of IFN-stimulated genes (ISG) such as IFN-induced tetratricopeptide repeat 5 (IFIT5). We unveil a new function of IFIT5 complex in degrading precursor miRNAs (pre-miRNA) that includes pre-miR-363 from the miR-106a-363 cluster as well as pre-miR-101 and pre-miR-128, who share a similar 5′-end structure with pre-miR-363. These suppressive miRNAs exerted a similar function by targeting EMT transcription factors in prostate cancer cells. Depletion of IFIT5 decreased IFNγ-induced cell invasiveness *in vitro* and lung metastasis *in vivo*. IFIT5 was highly elevated in high-grade prostate cancer and its expression inversely correlated with these suppressive miRNAs. Altogether, this study unveils a pro-metastatic role of the IFNγ pathway via a new mechanism of action, which raises concerns about its clinical application.

Significance: A unique IFIT5–XRN1 complex involved in the turnover of specific tumor suppressive microRNAs is the underlying mechanism of IFNγ-induced epithelial-to-mesenchymal transition in prostate cancer.

See related commentary by Liu and Gao, p. 1032

Introduction

IFNγ is first characterized as a cytokine associated with antivirus and antitumor activities during cell-mediated innate immune response (1, 2). Mechanistically, IFNs can activate JAK–STAT signaling pathway leading to the transcriptional activation of a variety of IFN-stimulated genes (ISG), resulting in diverse biologic responses (3). Among ISGs, IFN-induced tetratricopeptide repeat (IFIT) family members are highly inducible. They are viral RNA-binding proteins (4) and a part of antiviral defense mechanisms. Among IFIT orthologs, human IFIT1, IFIT2, and IFIT3 form a complex through the tetratricopeptide repeats (TPR) to degrade viral RNA. However, the functional role of IFIT5 is not fully understood because it acts solely as a monomer that can not only bind directly to viral RNA molecules via its convoluted RNA-binding cleft, but also endogenous cellular RNAs with a 5′-end phosphate cap, including transfer RNAs (tRNA; refs. 5, 6). In this study, we demonstrate a new function of IFIT5 in regulating miRNAs turnover.

miRNAs regulate approximately 60% of protein-coding genes via posttranscriptional suppression, mRNA degradation, or translation inhibition (7, 8). Many miRNAs associated with different stages of tumor development are regulated at transcriptional or posttranscriptional level (9). Unlike most eukaryotic protein genes, several miRNAs such as miR-106a-363 (10) and miR-17-92 are clustered together to generate a polycistronic primary transcript (11–13), which implies a complicated regulation of miRNA biogenesis. For example, miR-363 belongs to the polycistronic miR-106a-363 cluster containing six miRNAs. Unlike the other five miRNAs with similar seed sequences and functions as the oncogenic miR-17-92 cluster (14), the seed sequence of miR-363 is distinct from the rest of miRNAs, suggesting different function. Indeed, based on the specific interaction with IFIT5, miR-363 biogenesis is mediated by miRNA turnover, which appears to be a new function of IFIT5.

[1]Department of Urology, University of Texas Southwestern Medical Center, Dallas, Texas. [2]Department of Urology, The First Affiliated Hospital, Medical School of Xi'an Jiaotong University, Xi'an China. [3]Department of Bioengineering, University of Texas at Arlington, Arlington, Texas. [4]Institute of Biomembranes, Bioenergetics and Molecular Biotechnologies, National Research Council, Bari, Italy. [5]Department of Pathology, NYU Langone Medical Center, New York, New York. [6]Department of Pathology, University of Texas Southwestern Medical Center, Dallas, Texas. [7]Department of Microbiology and Immunology, Graduate Institute of Biomedical Sciences, College of Medicine, Chang Gung University, Taoyuan, Taiwan. [8]Department of Life Sciences, National Chung Hsing University, Taichung, Taiwan. [9]Department of Biotechnology, Kaohsiung Medical University, Kaohsiung, Taiwan, Republic of China.

Note: Supplementary data for this article are available at Cancer Research Online (http://cancerres.aacrjournals.org/).

Corresponding Author: Jer-Tsong Hsieh, University of Texas Southwestern Medical Center, Harry Hines Blvd., Dallas, TX 75390. Phone: 214-648-3988; Fax: 214-648-8786; E-mail: jt.hsieh@utsouthwestern.edu

doi: 10.1158/0008-5472.CAN-18-2207

Published OnlineFirst November 30, 2018; DOI: 10.1158/0008-5472.CAN-18-2207

Based on the mechanism of IFIT5-elicied miR-363 degradation, additional miRNAs such as miR-101 and miR-128 are subjected to IFIT5 complex and target several epithelial-to-mesenchymal transition (EMT) transcriptional factors. Clinically, loss of these miRNAs is associated with tumor grade of prostate cancer, which is inversely correlated with elevated IFIT5 mRNA level. However, IFIT5 mRNA expression is correlated with ZEB1 and Slug mRNA expression in prostate cancer specimens. Taken together, IFIT5 regulated by IFNγ is involved in unique miRNA degradation that can promote EMT, leading to prostate cancer metastasis.

Materials and Methods

Cell lines

Cells were obtained from ATCC: LAPC4 in Iscove DMEM containing 10% FBS; RWPE-1 in keratinocyte medium containing 10% FBS; LNCaP and PC3 in RPMI1640 medium containing 10% FBS. All the DAB2IP-KD and control (Con) prostate cell lines (such as RWPE1, PC3, and LAPC4) were described previously (15). Stable IFIT5-knockdown (KD; shIFIT5) and control (shCon) prostatic cell lines were generated from PC3, LAPC4-KD, RWPE1-KD, and C4-2Neo cell lines using pLKO-shIFIT5. Stable IFIT5-overexpressing (IFIT5) and control (Vec) cell lines were generated from LAPC4-Con, RWPE1-Con, and C4-2D2 cell lines using pcDNA3.1-3XFlag-IFIT5 plasmid from Dr. Collins (5). All these cell lines were used within 20 passages and authenticated with the short tandem repeat (STR) profiling by Genomic Core in UT Southwestern (UTSW) periodically and *Mycoplasma* testing was performed by MycoAlert Kit (Lonza Walkersville Inc.) every quarterly to ensure *Mycoplasma*-free.

In vitro transcription of pre-miRNA and RNA pull-down assay

The PCR-amplified DNA fragment of T7- precursor-miRNAs (pre-miRNA; Supplementary Table S1) was separated by 2% agarose gel electrophoresis and purified using Mermaid SPIN Kit (MP Biomedicals) then subjected to *in vitro* transcription assay using T7 High Yield RNA Synthesis Kit (New England Biolabs). The pre-miRNA molecules were treated with DNase I for 15 minutes at 25°C and purified by acid phenol–chloroform extraction and ethanol precipitation at −20°C for 1 hour. The molecular size and sequence of each purified precursor miRNA was confirmed by gel electrophoresis using 15% TBE-Urea gel and qRT-PCR, respectively.

The *in vitro* transcribed pre-miRNA was subjected to RNA pull-down assay using Pierce Magnetic RNA-Protein Pull-Down Kit (ThermoScientific). An approximate 100 pmol of pre-miRNA were incubated with 10X RNA Ligase reaction buffer, RNase inhibitor, Biotinylated Cytidine Bisphosphate, and T4 RNA ligase at 16°C for 16 hours. The biotinylated pre-miRNA was then purified and incubated with streptavidin magnetic beads for 30 minutes at room temperature. Whole cell lysates (200 μg) were incubated with the biotinylated pre-miRNA beads at 4°C for 1 hour. After elution, proteins–pre-miRNA complex was separated by SDS-PAGE using Bolt 4% to 12% Bis-Tris Plus gel and stained with Coomassie blue then subjected to LC/MS-MS analysis. For identifying the interaction between mutant pre-miR-363s (SS6Mut, DSMut) and IFIT5 or miRNA processing machinery, the proteins–pre-miRNA complex was subjected to Western blot analysis and blotted by using primary antibodies against IFIT5, Dicer, or Drosha proteins.

In vitro pre-miRNA degradation assay

The *in vitro* transcribed pre-miRNAs were incubated with recombinant IFIT5 protein and/or XRN1 (New England Biolab) at 37°C, then the RNA-containing buffer were collected at indicated time points and subjected to 15% TBE-Urea gel electrophoresis. To quantify the degradation of precursor miRNA, the 15% TBE-Urea gel was then stained with GelRed Nucleic Acid Gel Stains (VWR) and visualized under UV light in the AlphaImager device (Protein Simple). The RNA bands were quantified by Multiplex band analysis (AlphaView Software) and the rate of degradation was calculated from each time point normalized to time zero.

Migration and invasion assay

Cells ($4–10 \times 10^4$) in the serum-free medium were plated on the upper chamber (8-μm pore size) of Transwell (Corning) with or without Matrigel for invasion or migration assay, respectively, whereas bottom chamber contained medium supplemented with 10% FBS. After 5 days, cells in the bottom chamber were fixed by 4% paraformaldehyde, stained, and visualized under microscope. Quantification of migratory cells was carried out with Crystal Violet staining and measurement at OD_{555nm}. Each experiment was performed in triplicates.

Animal model

All animal work was approved by the Institutional Animal Care and Use Committee from UTSW. Stable clones of PC3-shCon or -shIFIT5 were infected with luciferase lentivirus. One million PC3 cells pretreated with vehicle (PBS) or IFNγ (20 ng/mL, 48 hours) were resuspended in 50 μL PBS and then injected into the tail vein of male SCID mice, followed by intravenous injection of IFNγ (5 ng/mL,) weekly for 4 weeks. At eighth-week post-injection, lung metastasis of PC3 tumor was observed by bioluminescent imaging (BLI) using IVIS system then lungs were excised, fixed in 10% formalin, paraffin-embedded, and stained with hematoxylin and eosin for pathologic identification of tumor nodules presented in the lung parenchyma.

Clinical specimens and *ex vivo* culture of patient-derived prostate cancer explants

A total of 41 prostate cancer specimens obtained from UT Southwestern Tissue Bank were collected from 6-mm core punch from radical prostectomy and examined by pathologist to determine tumor grade then subjected to RNA extraction and 12 fresh prostate cancer tissues were obtained from men undergoing radical prostatectomy at UT Southwestern University Hospital.

The *ex vivo* culture was performed as previously described (16). Briefly, fresh prostate cancer tissue was dissected into 1 mm^3 cube and placed on a Gelatin sponge (Novartis) bathed in RPMI1640 media supplemented with 10% heat-inactivated FBS, 100 units/mL penicillin–streptomycin, 0.01 mg/mL hydrocortisone, and 0.01 mg/mL insulin (Sigma). In addition, to the media, was added either vehicle, IFNγ (25 ng/mL) or IFNγ (100 ng/mL). Tissues were cultured at 37 °C for 48 hours then snap-freeze in liquid nitrogen for RNA purification. The Institutional Review Board of UTSW approved the tissue procurement protocol for this study and written informed consent was obtained from all patients.

Published OnlineFirst November 30, 2018; DOI: 10.1158/0008-5472.CAN-18-2207

Statistical analysis

Statistics analyses were performed by using GraphPad Prism software. Statistical significance was evaluated using Student *t* test. $P < 0.05$ or $P < 0.0001$ was considered a significant difference between compared groups and marked with an asterisk. The statistical association between miR-363, miR-101, miR-128, and IFIT5 expression among different grades of human prostate cancer was evaluated with regression correlation analysis.

Results

The specific regulation of miR-363 expression

IFNγ is known to modulate cancer immunity and increase cytotoxicity. In addition, we observed that IFNγ was able to induce the expression of Slug and ZEB1, both are potent EMT transcription factors, in prostate cancer cell lines C4-2 (Fig. 1A) and PC3 cells (Supplementary Fig. S1A) in a dose-dependent manner. In contrast, Disabled homolog 2–interacting protein (DAB2IP) protein expression was reduced in treated cells (Fig. 1A; Supplementary Fig. S1A). We have previously identified DAB2IP as an EMT inhibitor in prostate cancer (15, 17). Thus, we believe that the mechanism of IFNγ-induced EMT is mediated through DAB2IP-regulated pathway. Because emerging evidence demonstrates a critical role of miRNA in EMT process, we decided to profile miRNA between DAB2IP-positive and -KD cells. From miRNA microarray screening (Supplementary Fig. S1B), a significant reduction of miR-363 (1176 folds decrease) was detected in DAB2IP-KD cells. The

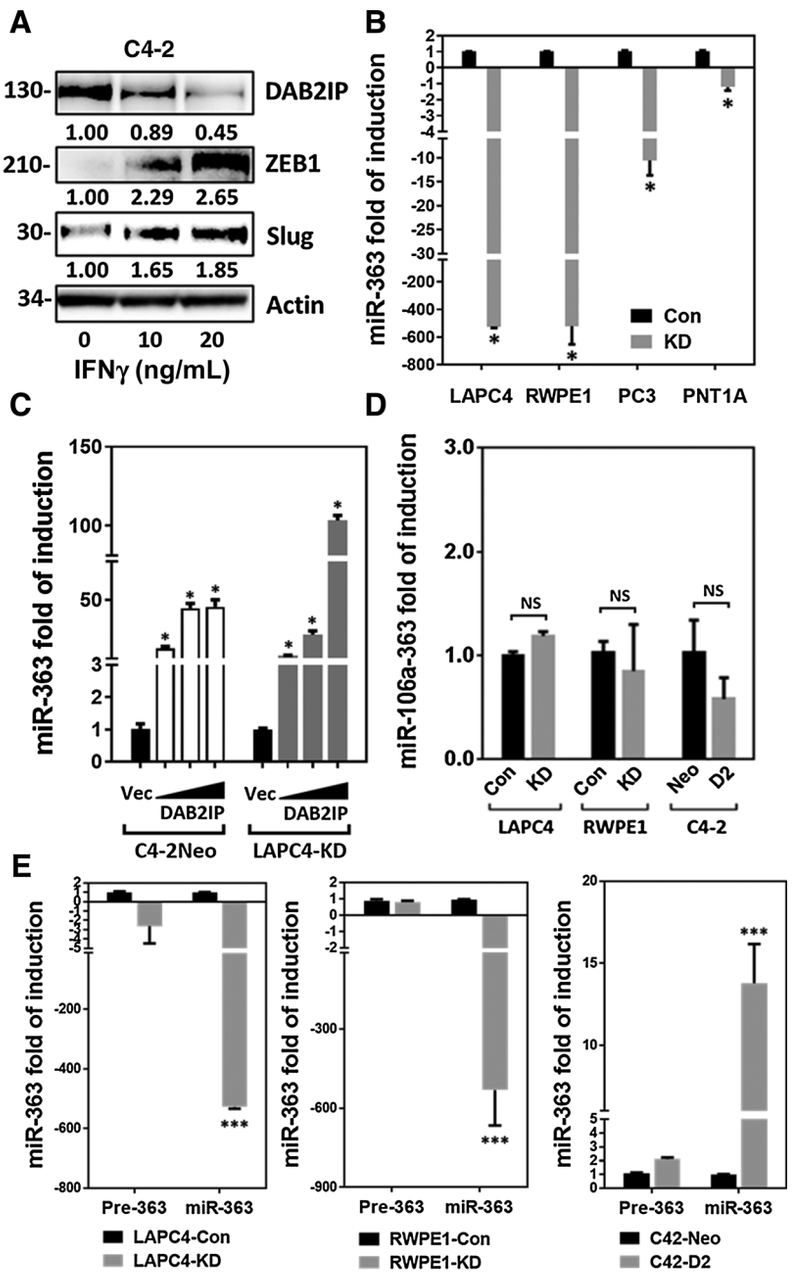

Figure 1.
The effect of DAB2IP on miR-363 expression in prostate cell lines. **A,** Induced expression of DAB2IP, ZEB1, and Slug protein level in C42 cells after treated with IFNγ for 48 hours. **B,** Expression levels of miR-363 in DAB2IP-KD prostate cell lines after normalizing to the Con cell of each cell line pair. *, $P < 0.05$. **C,** Induction of miR-363 by ectopic expression of DAB2IP in C4-2Neo and LAPC4-KD cell lines. Fold change of miR-363 levels were normalized to vector control. *, $P < 0.05$. **D,** Expression levels of primary miR-106a-363 in DAB2IP-positive and -negative sublines after normalizing to the Con cell of each cell line pair. NS, no significant differences. **E,** Expression levels of precursor miR-363 and mature miR-363 in DAB2IP-positive and -negative cells after normalizing to the control vector of each cell line pair. ***, $P < 0.0001$. Quantitative qRT-PCR data of miR-363 expression level were analyzed using ΔC_t (C_t value normalized to internal snord95 miRNAs) and $\Delta\Delta C_t$ (difference between the ΔC_t of control and each experimental group) values to obtain the fold change after normalizing with vector control.

Published OnlineFirst November 30, 2018; DOI: 10.1158/0008-5472.CAN-18-2207

downregulation of miR-363 in DAB2IP-KD cells was further validated in immortalized normal prostatic epithelial cell (RWPE1 and PNT1A) and prostate cancer lines (LAPC-4 and PC3; Fig. 1B). Ectopic expression of DAB2IP in C4-2Neo or LAPC4-KD cells (Fig. 1C) was able to induce mature miR-363 levels, indicating that DAB2IP could modulate miR-363 expression.

miR-363 is located in the polycistronic miR-106a-363 cluster that is first transcribed into a single primary miRNA containing the entire sequence of the cluster genes. We therefore examined

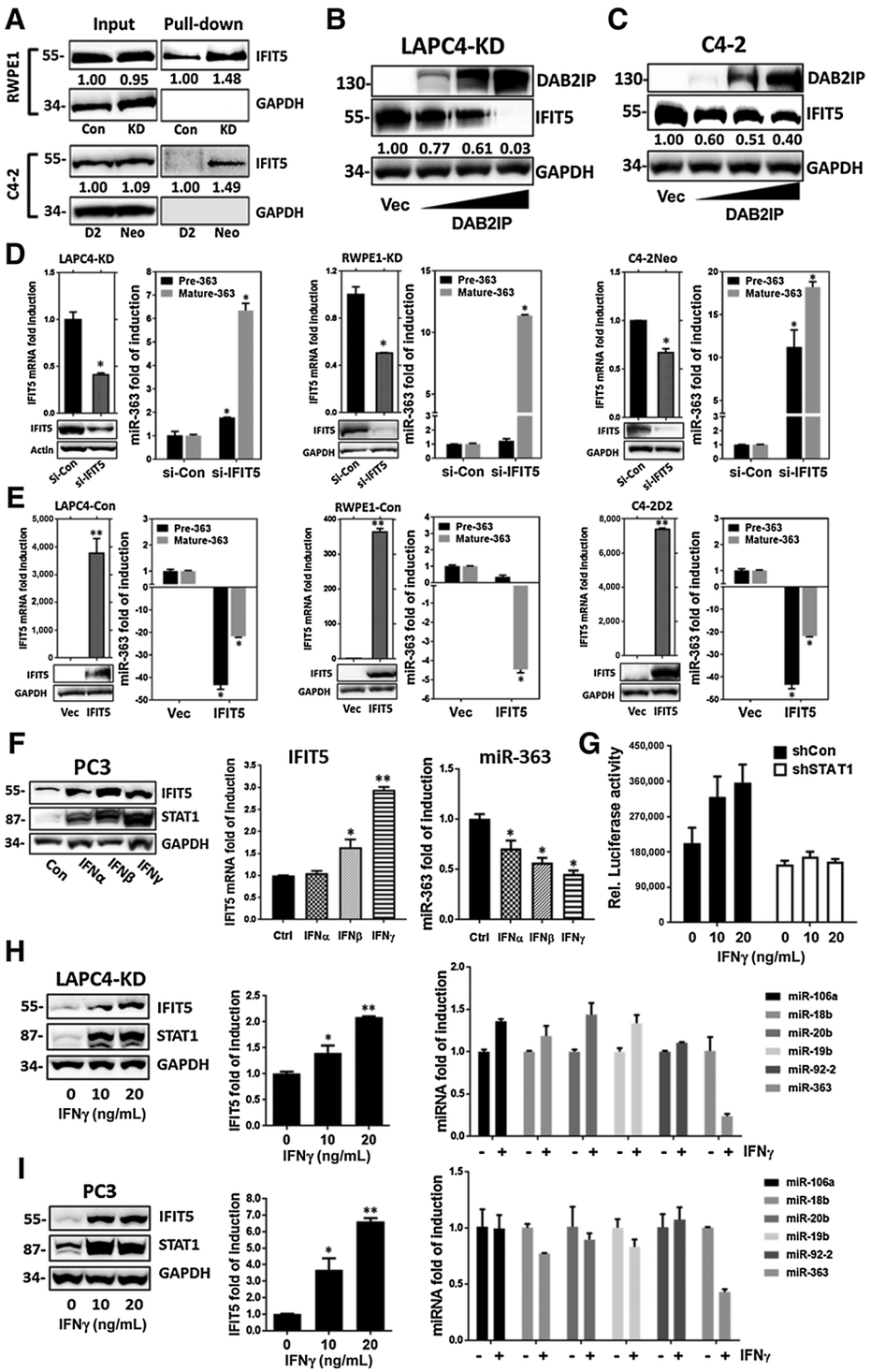

Figure 2.

The impact of IFIT5 on miR-363 maturation from the miR-106a-363 cluster. **A,** The interaction between IFIT5 protein and pre-miR-363 in DAB2IP-positive and -negative cells using RNA pull-down assay. **B** and **C,** Suppression of IFIT5 protein expression by ectopic transfecting DAB2IP into LAPC4-KD (**B**) and C4-2Neo (**C**) cells after normalizing with the control vector (Vec). **D,** Expression levels of precursor and mature miR-363 in IFIT5-siRNA KD (si-IFIT5) LAPC4-KD, RWPE1-KD, and C4-2Neo cells after normalizing to control siRNA (si-Con; *, $P < 0.05$). **E,** Expression levels of precursor and mature miR-363 in IFIT5-overexpressing (IFIT5) LAPC4-Con, RWPE1-Con, and C4-2D2 cells after normalizing to control vector (Vec; *, $P < 0.05$). **F,** Left and middle, induction of IFIT5 protein and mRNA level by IFNα, IFNβ, and IFNγ treatment for 48 hours in PC3 cells, compared with vehicle control. *, $P < 0.05$. Right, expression level of miR-363 in PC3 cells treated with IFNα, IFNβ, and IFNγ for 48 hours after normalizing to vehicle control. *, $P < 0.05$. **G,** IFNγ-induced IFIT5 promoter activity in PC3 cells with shRNA KD of STAT1 (shSTAT1), compared with control shRNA (shCon). Relative (Rel.) luciferase activity was normalized with protein concentration. **H** and **I,** Left and middle, dose-dependent induction of IFIT5 protein and mRNA level in LAPC4-KD and PC3 cells treated with IFNγ for 48 hours, compared with vehicle control. *, $P < 0.05$; **, $P < 0.0001$. Right, induction levels of mature miRNAs (miR-106a, miR-18b, miR-20b, miR-19b-2, miR-92a-2, and miR-363) in LAPC4-KD and PC3 cells treated with IFNγ (+, 20 ng/mL) for 48 hours, compared with vehicle control (−). *, $P < 0.05$. All quantitative data of IFIT5 mRNA or miRNA expression level were analyzed using ΔC_t (C_t value normalized to internal 18S RNA or snord95 miRNA) and $\Delta\Delta C_t$ (difference between the ΔC_t of control and experimental groups) values to obtain the fold change after normalizing with control group.

Published OnlineFirst November 30, 2018; DOI: 10.1158/0008-5472.CAN-18-2207

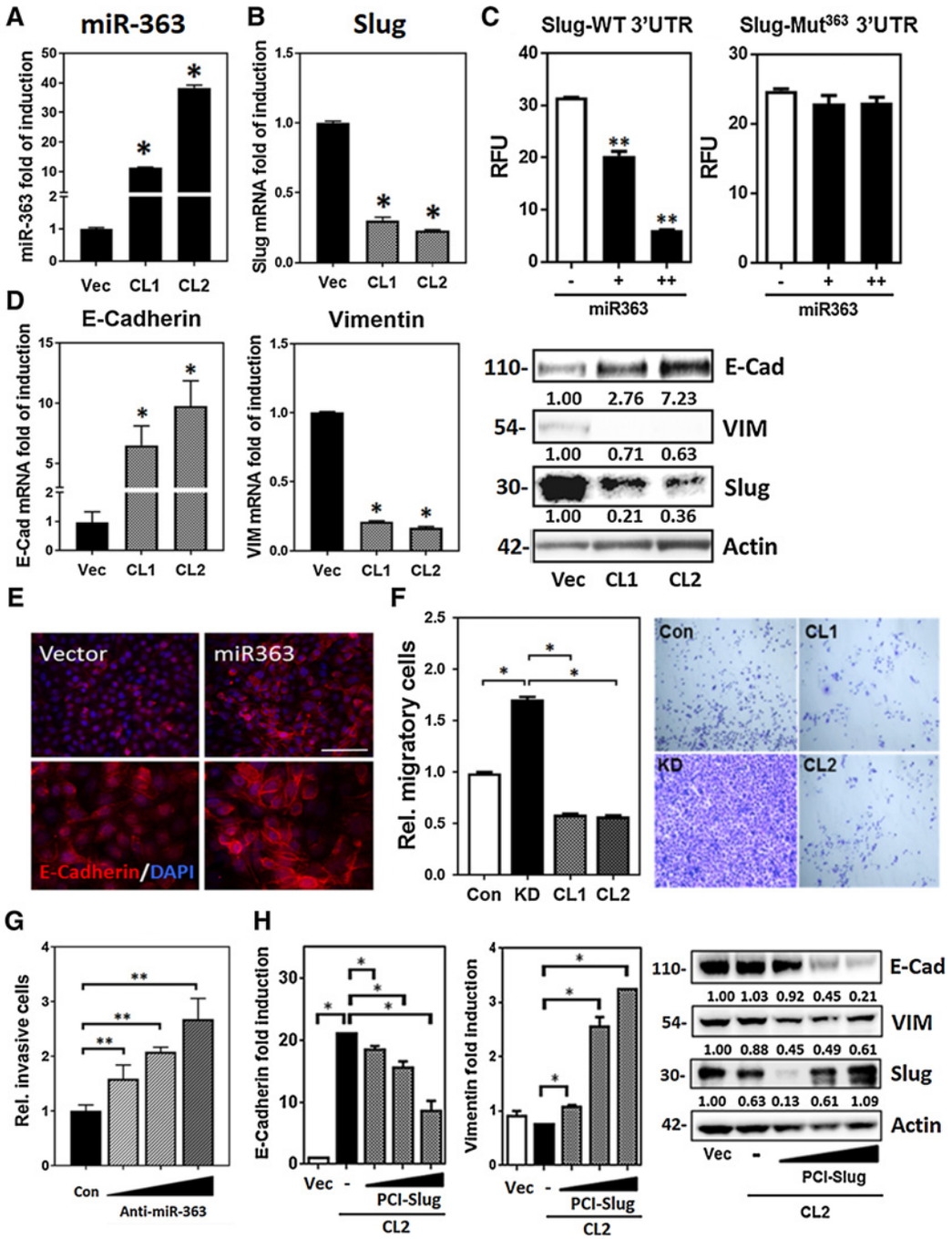

Figure 3.

The inhibitory effect of miR-363 on EMT by targeting Slug. **A,** Upregulation of miR-363 in RWPE1-KD cells transfected with pCMV-miR-363 plasmid after normalizing with vector control. *, $P < 0.05$. **B,** Reduction of Slug mRNA expression and protein level in miR-363–expressing RWPE1-KD cells after normalizing to vector control. *, $P < 0.05$. CL, stable clone of miR-363-expressing RWPE1-KD cells. **C,** Luciferase reporter assay in RWPE1-KD cells cotransfected with psiCHECK2-slug-WT 3′UTR or psiCHECK2-Slug Mut363 3′UTR and pCMV-miR363 or empty vector (−). Luciferase activity unit is plotted as *Renilla* to Firefly luciferase activity (RFU). Each bar represents mean ± SD of four replicated experiments. **, $P < 0.0001$. **D,** Induced mRNA and protein expression of E-cadherin, Slug, and vimentin in miR-363–expressing RWPE1-KD cells after normalizing to vector control. *, $P < 0.05$. **E,** Immunofluorescence staining of E-cadherin protein expression in miR-363–expressing RWPE1-KD cells, compared with vector control. **F,** Transwell migration assay in miR-363–expressing RWPE1-KD cells. Transmigrated RWPE1 cells were observed by crystal violet staining and quantified at OD 555 nm. Each bar represents mean ± SD of three replicated experiments. *, $P < 0.05$. **G,** Transwell invasion assay in RWPE1-Con transfected with different dose of anti-miR-363. Transmigrated cells were stained with crystal violet and quantified at OD 555 nm. Each bar represents mean ± SD of three replicated experiments. **, $P < 0.05$. **H,** E-cadherin and vimentin mRNA and protein expression level after restoration of slug in miR-363–expressing RWPE1-KD cells, compared with vector control (*, $P < 0.05$). All quantitative data of mRNA or miRNA expression level were analyzed using ΔC_t (C_t value normalized to internal 18S RNA or snord95 miRNA) and $\Delta\Delta C_t$ (difference between the ΔC_t of control vector and experimental groups) values to obtain the fold change after normalizing with vector control.

Published OnlineFirst November 30, 2018; DOI: 10.1158/0008-5472.CAN-18-2207

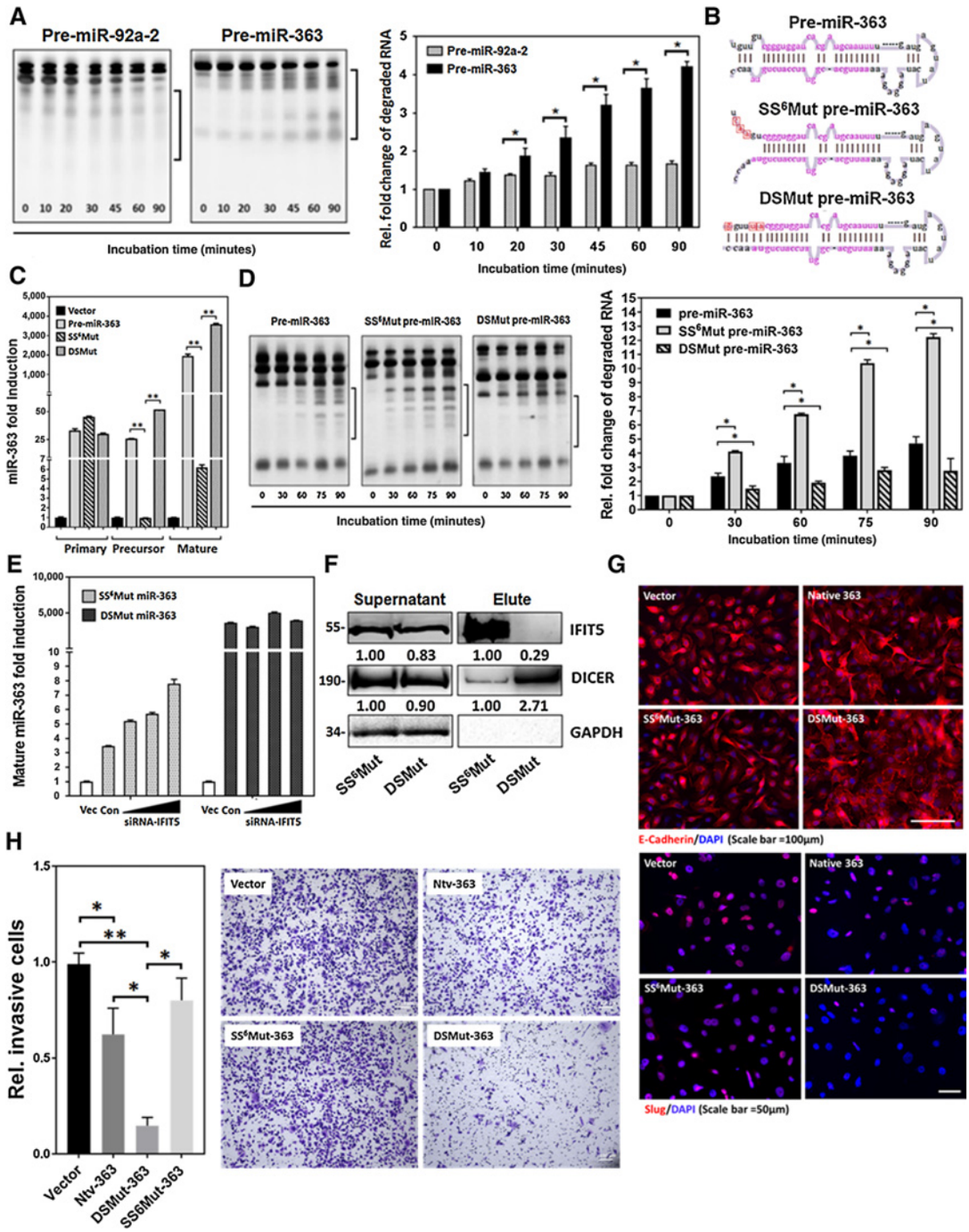

Figure 4.

The effect of IFIT5 on pre-miR-363 degradation *in vitro*. **A,** Time-dependent change of degraded pre-miR-92a-2 and pre-miR-363 fragments (bracket) after incubation with IFIT5 protein complex at 37°C normalized with 0 min. *, $P < 0.05$. **B,** Mutation of nucleotides (red box) for generating 5′-end six nucleotides single-stranded pre-miR-363 (SS6Mut pre-miR-363) and blunt 5′-end double stranded pre-miR-363 (DSMut pre-miR-363). Both mature miR-363 and miR-363* sequences are shown in pink. **C,** Expression levels of primary, precursor, and mature miR-363 in LAPC4-KD cells transfected with Native, SS6Mut, or DSMut pre-miR-363 plasmids for 24 hours after normalizing with the vector control. **D,** Time-dependent degradation of native, SS6Mut, and DSMut pre-miR-363 fragments (bracket) after incubation with IFIT5 protein at 37°C; each time point was normalized with 0 min. *, $P < 0.05$. **E,** Dose-dependent induction of mature miR-363 in cells transfected with SS6Mut pre-miR-363 or DSMut pre-miR-363 plasmids and IFIT5 siRNA after normalizing with the control vector (Vec). Con, control siRNA. **F,** Interaction between IFIT5 protein and SS6Mut or DSMut pre-miR-363 RNA molecules using RNA pull-down assay. **G,** Immunofluorescence staining of E-cadherin and Slug in mutant pre-miR-363–overexpressed RWPE1-KD cells, compared with vector control. **H,** The effect of Native, DSMut-, or SS6Mut-pre-miR-363 on cell invasion in PC3 cells. Cells invaded at the lower bottom at the Transwell were stained with crystal violet and counted. Each bar represents mean ± SD of nine fields of counted cell numbers. *, $P < 0.05$; **, $P < 0.0001$. All quantitative data of miR-363 expression level were analyzed using ΔC_t (C_t value normalized to internal snord95 miRNA) and $\Delta\Delta C_t$ (difference between the ΔCt of control vector and experimental groups) values to obtain the fold change after normalizing with vector control.

Published OnlineFirst November 30, 2018; DOI: 10.1158/0008-5472.CAN-18-2207

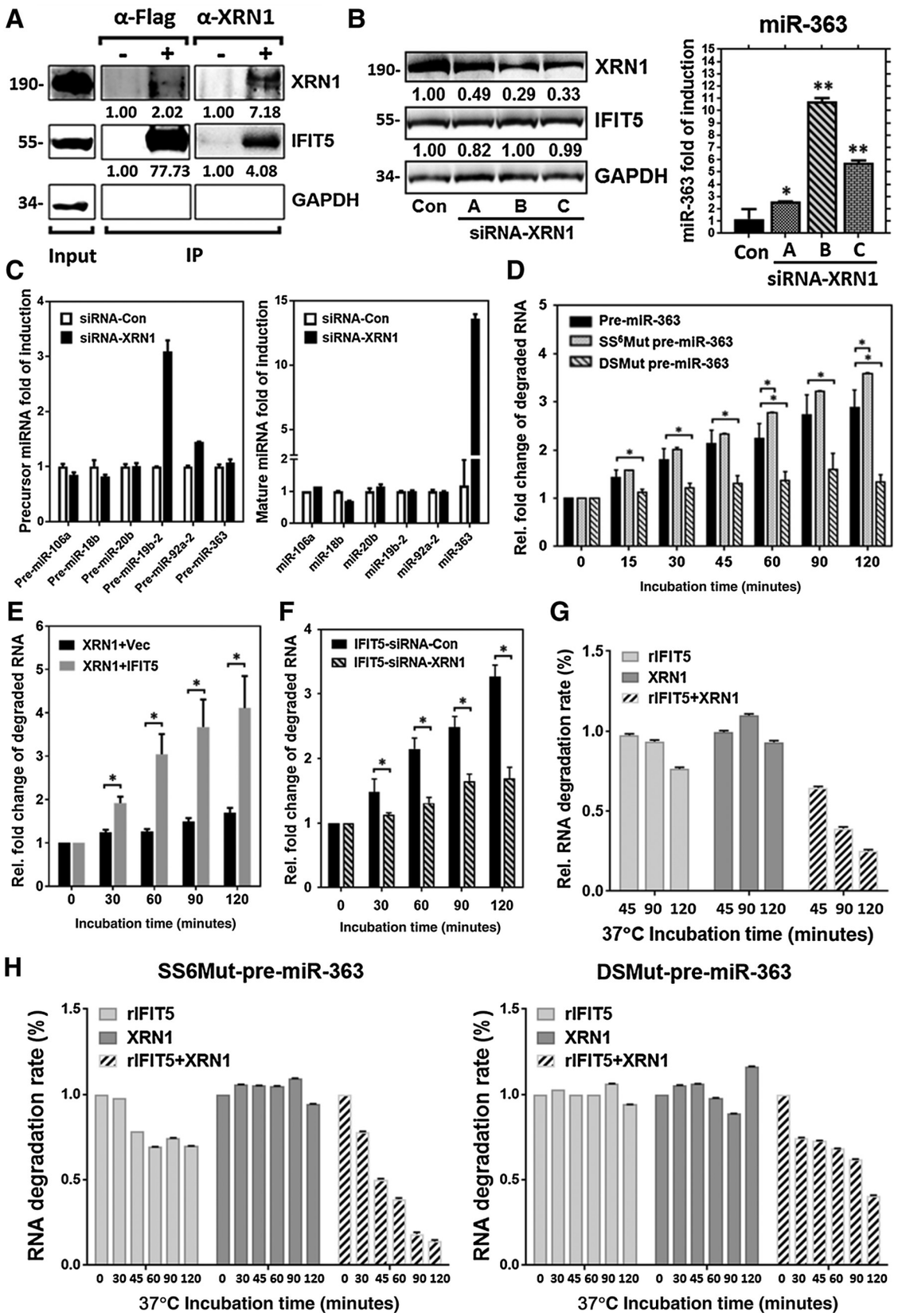

Published OnlineFirst November 30, 2018; DOI: 10.1158/0008-5472.CAN-18-2207

the effect of DAB2IP on the expression levels of primary transcript of miR-106a-363. In contrast to the significant downregulation of mature miR-363 in DAB2IP-KD cells, the expression levels of either primary miR-106a-363 (Fig. 1D) or pre-miR-363 (Fig. 1E) were similar between DAB2IP-positive and -KD cells. Noticeably, among the miRNA members in the miR-106a-363 cluster, only mature miR-363 levels dramatically decreased in DAB2IP-KD cells (i.e., LAPC4-KD and RWPE-1-KD; Fig. 1E; Supplementary Fig. S1C and S1D). However, only mature miR-363 levels increased significantly in C4-2D (Fig. 1E; Supplementary Fig. S1E) with ectopic expression of DAB2IP. These findings indicate that DAB2IP specifically regulates miR-363 maturation from the miR-106a-363 cluster.

Effect of IFIT5 on the biogenesis of miR-363

To elucidate the machinery responsible for miR-363 maturation process, the protein candidates were pulled down by synthetic pre-miR-363 RNA and subjected to LC/MS-MS analysis. IFIT5 (Supplementary Table S2) is consistently showing higher affinity with pre-miR-363 among all three DAB2IP-negative cell lines (LAPC-KD, RWPE1-KD, and C4-2Neo) when compared with DAB2IP-positive cell lines, LAPC4-Con, RWPE1-Con, and C4-2D2, respectively. Moreover, IFIT5 appeared to be a viral-RNA-binding protein, which match with our criteria while searching for a RNA-interacting protein as a potential candidate from the pre-miR-363 RNA pull-down results. The steady-state levels of IFIT5 mRNA and protein were inversely correlated with DAB2IP (Supplementary Fig. S2A). IFIT5 has not been shown to bind to miRNAs; therefore, the interaction between pre-miR-363 and IFIT5 was confirmed in DAB2IP-negative and -positive prostate cancer cell lines (Fig. 2A). This inhibitory effect of DAB2IP on IFIT5 expression was also demonstrated by the ectopic expression of DAB2IP in LAPC4-KD (Fig. 2B), C4-2 (Fig. 2C), and LNCaP cells (Supplementary Fig. S2B).

To determine the role of IFIT5 in miR-363 maturation, we used siRNA to KD IFIT5 in DAB2IP-negative cells. In LAPC4-KD cells treated with several IFIT5 small-interfering RNA (siRNA), the elevated levels of mature miR-363 were detected, which was inversely correlated with the reduction of the endogenous IFIT5 mRNA levels (Supplementary Fig. S2C). Because IFIT5-C siRNA exhibited high efficiency, this siRNA was further tested with RWPE1-KD cells and data showed a significant elevation of mature miR-363 (Supplementary Fig. S2D). Despite the significantly elevated mature miR-363 in IFIT5-siRNA KD cells (Fig. 2D; Supplementary Fig. S2E), the levels of mature miR-106a, miR-18b, miR-20b, miR-19b-2, miR-92a-2 remained relatively unchanged (Supplementary Fig. S2F). However, we ectopically expressed IFIT5 in DAB2IP-positive cells and observed a significant reduction of mature miR-363 levels but not other mature miRNAs from the same cluster (Fig. 2E; Supplementary Fig. S2G). Overall, our finding indicates that IFIT5 can specifically inhibit miR-363 maturation from the miR-106a-363 cluster.

Effect of IFNs on the biogenesis of miR-363 in prostate cancer cells

Knowing IFIT5 as a typical ISG, we further confirmed that all IFNs can induce IFIT5 in PC3 cells (Fig. 2F). Meanwhile, a significant reduction of miR-363 was observed under the same condition (Fig. 2F). Among three IFNs, the type II IFN, IFNγ, has the most potent effect on inducing IFIT5 mRNA and suppressing miR-363. We therefore, used IFNγ to examine its impact on IFIT5 downstream target miRNAs. We first identified that the induction of IFIT5 mRNA by IFNγ was the result of transcriptional activation mediated by STAT1 signaling using IFIT5 gene promoter construct (Fig. 2G). Moreover, a dose-dependent induction of IFIT5 protein and mRNA by IFNγ was detected in LAPC4-KD and PC3 cells (Fig. 2H and I) and significantly reduce mature miR-363 levels compared with other miRNAs in miR-106a-363 cluster (Fig. 2H and I). These data support a key mediator role of IFIT5 in IFNγ-mediated miR-363 suppression. Noticeably, the other member of IFIT family, such as IFIT1, was absent in PC3 cell after IFNγ treatment in contrast to RWPE1 cell (Supplementary Fig. S2H), implying IFIT5 plays a unique role in prostate cancer progression.

The functional role of miR-363 in EMT

Based on the predicted sequences and gene profiling, Slug/SNAI2 mRNA appears to be a potential target gene of miR-363. By transfecting miR-363 vector into DAB2IP-KD cells, the suppression of Slug/SNAI2 mRNA levels was detected in miR-363 expressing cells compared with controls (Fig. 3A and B; Supplementary Fig. S3A). Using both wild-type Slug/SNAI2 3′UTR (Slug-WT3′UTR) and mutant Slug/SNAI2 3′UTR (Slug-Mut^{363}3′UTR) luciferase reporter genes, a significant reduction of the Slug-WT3′UTR but not the Slug-Mut^{363}3′UTR activity was detected in RWPE-1-KD (Fig. 3C) and LAPC4-KD cells (Supplementary Fig. S3B).

Slug/SNAI2 is known to promote EMT by suppressing E-cadherin. As expected, an elevation of E-cadherin mRNA and protein was observed in miR-363 overexpressing RWPE1-KD (Fig. 3D and E) and LAPC4-KD cells (Supplementary Fig. S3C). In contrast, vimentin, a mesenchymal marker, was suppressed (Fig. 3D; Supplementary Fig. S3C). Functionally, ectopic expression of miR-363 was able to reduce cell migration in RWPE1-KD (Fig. 3F) and LAPC4-KD cells (Supplementary Fig. S3D). Noticeably, cells collected from the bottom chamber of a

Figure 5.

Interaction between XRN1 with IFIT5 leading to pre-miR-363 degradation *in vitro*. **A,** Interaction between IFIT5 and XRN1 proteins using immunoprecipitation by Flag and XRN1 antibodies, respectively. **B,** Left, KD of XRN1 in LAPC4-KD cells using siRNA. Right, induction of mature miR-363 in LAPC4-KD cells transfected with XRN1 siRNA after normalizing with the control siRNA (Con). *, $P < 0.05$; **, $P < 0.0001$. **C,** Expression levels of precursor and mature miRNAs (miR-106a, miR-18b, miR-20b, miR-19b-2, miR-92a-2, and miR-363) in XRN1-KD (siRNA-XRN1) LAPC4-KD cells after normalizing with the control siRNA (siRNA-Con). **D,** Time-dependent change of degraded native, SS6Mut, and DSMut pre-miR-363 fragments after incubation with immunoprecipitated XRN1 protein at 37°C after normalizing with 0 minute. *, $P < 0.05$. **E,** Time-dependent change of degraded SS6Mut pre-miR-363 fragments after incubation with immunoprecipitated XRN1 alone (XRN1+Vec) or XRN1-IFIT5 complex (XRN1+IFIT5) at 37°C after normalizing with 0 minute. *, $P < 0.05$. **F,** Time-dependent change of degraded SS6Mut pre-miR-363 after incubation with the immunocomplex derived from cells transfected with IFIT5 and control siRNA (IFIT5+siRNA-Con) or XRN1 siRNA (IFIT5+siRNA-XRN1) at 37°C after normalizing with 0 minute. *, $P < 0.05$. **G,** Degradation of native pre-miR-363 after incubation with recombinant IFIT5 protein (rIFIT5), XRN1 enzyme (XRN1), or combination of XRN1 and rIFIT5 at 37°C after normalizing with 0 minute. **H,** Degradation of SS6Mut- or DSMut-pre-miR-363 after incubation with rIFIT5, XRN1, or combination of XRN1 and rIFIT5 at 37°C after normalizing with 0 minute. Quantitative data of miR-363 expression level were analyzed using ΔC_t (C_t value normalized to internal snord95 miRNA) and $\Delta\Delta C_t$ (difference between the ΔC_t of control vector and experimental groups) values to obtain the fold change after normalizing with vector control.

Published OnlineFirst November 30, 2018; DOI: 10.1158/0008-5472.CAN-18-2207

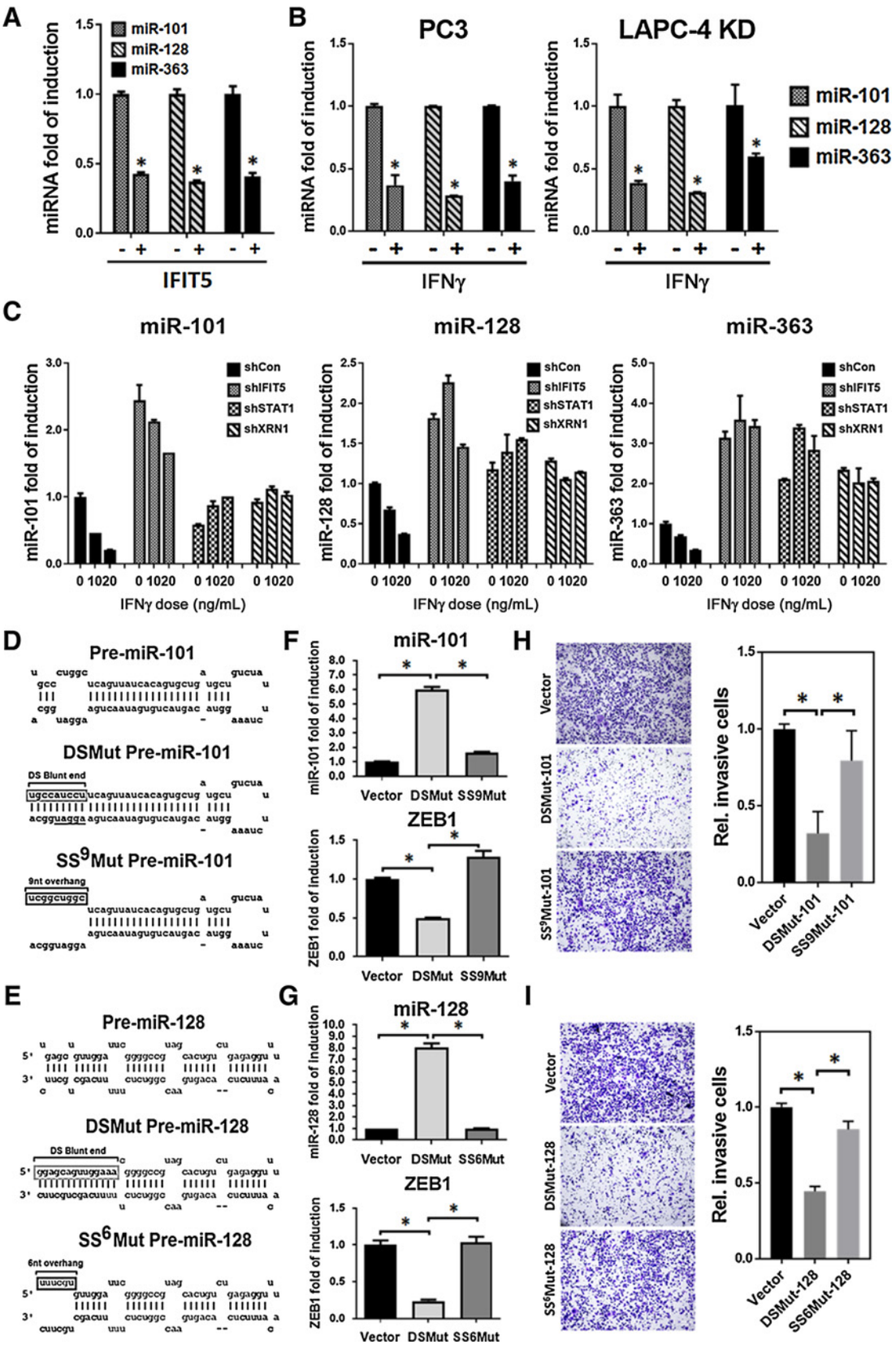

Transwell exhibited lower miR-363 levels than those from the upper chamber (Supplementary Fig. S3D). In contrast, inhibition of miR-363 in RWPE1-Con (Fig. 3G), Du145, and C4-2 cells (Supplementary Fig. S3E) increased cell invasion and migration, respectively. Moreover, restored Slug/SNAI2 levels in miR-363–expressing cells were resulted in a dose-dependent reduction of E-cadherin and elevation in vimentin in RWPE1-KD (Fig. 3H) and LAPC4-KD cells (Supplementary Fig. S3F). These data indicate that miR-363 can suppress EMT by targeting Slug in prostate cancer.

The mechanism of IFIT5 on miR-363 turnover at precursor level

IFIT5 has been suggested to suppress virus replication by targeting the 5′-phosphate end of single-stranded viral RNAs for rapid turnover (6). Thus, we examined whether IFIT5 has a direct impact on the stability of pre-miR-363. In fact, pre-miR-363 RNA prepared from *in vitro* transcription was relatively stable at 37°C (Supplementary Fig. S4A) but quickly degraded in the presence of IFIT5 protein complex (Supplementary Fig. S4A), indicating that the degradation of pre-miR-363 is accelerated by the IFIT5 protein complex. To examine the specificity of IFIT5 in the acceleration of pre-miR-363 degradation, we found no significant change for *in vitro* degradation rate of pre-miR-92a-2 (immediate adjacent to miR-363) under the same condition (Fig. 4A). Previous studies (4, 5) indicate that IFIT5 protein binds to viral RNA molecules at either 5′-phosphate cap or 5′-tri-phosphate group. By comparing the 5′-end structure between pre-miR-92a-2 and pre-miR-363, we hypothesized that a single nucleotide (uracil) overhang in pre-miR-363, in contrast to the double-stranded blunt end in pre-miR-92a-2, is critical for IFIT5 recognition. Therefore, we generated two mutant pre-miR-363 constructs: one with 5′-end six nucleotides single-stranded overhang (SS^6Mut) and the other with double-stranded blunt end (DSMut; Fig. 4B) to test their stabilities. The *in vivo* result (Fig. 4C; Supplementary Fig. S4B) indicated that the expression levels of pre-miR363 or mature miR-363 derived from SS^6Mut were significantly lower than those from native or DSMut form (Fig. 4C; Supplementary Fig. S4B), indicating that the 5′-end structure of pre-miR-363 dictates the stability of miR-363 maturation. By determining the *in vitro* degradation rates of native, pre-SS^6Mut- and pre-DSMut -miR-363 RNA molecules, as we expected, pre-SS^6Mut-miR-363 was very sensitive to IFIT5 whereas pre-DSMut-miR-363 was the most resistant one (Fig. 4D). Furthermore, we observed a steady elevation of SS^6Mut -derived mature miR-363 level in a dose-dependent manner in the presence of an incremental IFIT5 siRNA, whereas the expression of mature DSMut-miR-363 was not impacted by IFIT5 siRNA (Fig. 4E). Meanwhile, using RNA pull-down assay, pre-SS^6Mut-miR-363 exhibited higher affinity to IFIT5 protein than pre-DSMut -miR-363 (Fig. 4F). Noticeably, the biogenesis of these artificial constructs is similar to native one (Fig. 4C; Supplementary Fig. S4B). As expected, all these precursor constructs exhibited low binding affinity to Drosha (Supplementary Fig. S4C), compared with the primary transcript containing both miR-92a-2 and miR-363 (Pri-92a-2+363). However, pre-DSMut-miR-363 exhibited the highest binding affinity to DICER among native and pre-SS^6Mut-miR-363 (Supplementary Fig. S4C), suggesting IFIT5 could prevent Dicer from binding to pre-miR-363. Knowing the high stability of pre-DSMut-miR-363 *in vivo*, it exhibited more potent effect on inhibiting EMT (Supplementary Fig. S4D) evidenced by elevated E-cadherin and reduced Slug protein expression in RWPE1 (Fig. 4G) and PC3 cells (Supplementary Fig. S4E). Also, DSMut exhibited a greater impact on diminishing PC3 and LAPC4-KD cell invasion (Fig. 4H; Supplementary Fig. S4F) and migration (Supplementary Fig. S4F). These data conclude that IFIT5 recognizes the unique 5′-end overhanging structure of pre-miR-363 for its degradation.

To further demonstrate the specificity of this unique 5′-end structure of pre-miRNA, we also generated a mutant construct of pre-miR-92a-2 with single nucleotide at 5′-overhang (SS^1Mut pre-miR-92a-2; Supplementary Fig. S4G), which is similar to the 5′-end of pre-miR-363 (Fig. 4B). Using RNA pull-down assay, we observed an increased interaction between SS^1Mut pre-miR-92a-2 and IFIT5 protein, compared with native pre-miR-92a-2 (Supplementary Fig. S4G). Moreover, the degradation rate of pre-SS^1Mut-miR-92a-2 increased in the presence of IFIT5 complex, compared with that of pre-miR-92a-2 (Supplementary Fig. S4H). Thus, the 5′-end overhanging structure of pre-miRNAs dictates IFIT5-elicited miRNA turnover.

The role of XRN1 in IFIT5-mediated miR-363 turnover

Although IFIT5 can elicit miR-363 turnover, IFIT5 does not possess ribonuclease activity. To determine whether a ribonuclease is associated with the IFIT5–pre-miR-363 complex, we further examined LC/MS-MS results derived from pre-miR-363 pull-down protein candidates and identified an exoribonuclease candidate-XRN1. XRN1 is known to regulate mRNA stability via cleavage of de-capped 5′-monophosphorylated mRNA (18, 19) and a recent study also implied its potential role in miRNA turnover (20). Indeed, an interaction was observed between IFIT5 and XRN1 protein in LAPC4-Con cells transfected with Flag-tagged IFIT5 (Fig. 5A). Meanwhile, an interaction between endogenous IFIT5 and XRN1 protein is also observed in PC3 cells

Figure 6.

The impact of IFIT5–XRN1 on pre-miRNA degradation and EMT of prostate cancer cells. **A,** Expression level of mature miR-101, miR-128, and miR-363 in IFIT5-overexpressed (+) PC3 cells, compared with vector control (−) *, $P < 0.05$. **B,** Expression level of miR-101, miR-128, and miR-363 in PC3 and LAPC4-KD cells treated with IFNγ (+), compared with control vector (−) *, $P < 0.05$. **C,** Expression level of miR-101, miR-128, and miR-363 in PC3 cells treated with IFNγ after KD of IFIT5 (shIFIT5), STAT1 (shSTAT1), or XRN1 (shXRN1), compared with vector control (shCon). **D,** Mutation of nucleotides (box) for generating blunt 5′-end double-stranded pre-miR-101 (DSMut pre-miR-101) and 5′-end nine nucleotides single-stranded pre-miR-101 (SS9Mut pre-miR-101). Gray, mature miR-101 and miR-101* sequence. **E,** Mutation of nucleotides (box) for generating blunt 5′-end double-stranded pre-miR-128 (DSMut pre-miR-128) and 5′-end six nucleotides single-stranded pre-miR-128 (SS6Mut pre-miR-128). Gray, mature miR-128 and miR-128* sequence. **F,** The effect of DSMut or SS9Mut pre-miR-101 on the expression level of mature miR-101 and ZEB1 mRNA (*, $P < 0.05$) after normalizing to vector control. **G,** The effect of DSMut or SS6Mut pre-miR-128 on the expression level of mature miR-128 and ZEB1 mRNA. *, $P < 0.05$. **H,** The effect of DSMut or SS9Mut pre-miR-101 on the cell invasion in PC3 cells. Cells invaded at the lower bottom at the Transwell were stained with crystal violet and counted. Each bar represents mean ± SD of nine fields of counted cell numbers. *, $P < 0.05$. **I,** The effect of DSMut or SS6Mut pre-miR-128 on the cell invasion in PC3 cells. Cells invaded at the lower bottom at the Transwell were stained with crystal violet and counted. Each bar represents mean ± SD of nine fields of counted cell numbers. *, $P < 0.05$. All quantitative data of miRNA or mRNA expression level were analyzed using ΔC_t (C_t value normalized to internal snord95 miRNA or 18S RNA) and $\Delta\Delta C_t$ (difference between the ΔC_t of control and experimental groups) values to obtain the fold change after normalizing with control.

Published OnlineFirst November 30, 2018; DOI: 10.1158/0008-5472.CAN-18-2207

(Supplementary Fig. S5A). Also, the expression levels of miR-363 were correlated with the diminished level of XRN1 protein (Fig. 5B; Supplementary Fig. S5B). Similar to IFIT5-KD, data from XRN1-KD cells clearly demonstrated that only mature miR-363 exhibited a significant accumulation whereas the levels of other mature miRNAs (miR-106a, miR-18b, miR-20b, miR-19b-2, and miR-92a-2) remained relatively unchanged (Fig. 5C). By incubating XRN1 immunocomplex (Supplementary Fig. S5C) with native, SS^{6}Mut or DSMut pre-miR-363 RNA *in vitro*, a significantly increased degradation of both native and pre-SS^{6}Mut-miR-363 was detected in a time-dependent manner, whereas pre-DSMut-miR-363 levels remained relatively unchanged (Fig. 5D; Supplementary Fig. S5C), implying that the IFIT5 binding structure in the 5′-end of pre-miR-363 is critical for recruiting XRN1. In addition, by increasing IFIT5 expression in XRN1-positive LAPC4-Con cells, XRN1–IFIT5 immunocomplex apparently increased the *in vitro* degradation of SS^{6}Mut-pre-miR-363 compared with control (XRN1 alone; Fig. 5E; Supplementary Fig. S5D). However, knocking down XRN1 in IFIT5-overexpressing LAPC4-Con cells diminished the *in vitro* degradation rate of pre-SS^{6}Mut-miR-363 after incubation with IFIT5 (Fig. 5F; Supplementary Fig. S5E). These findings provide further evidence for the specific function of IFIT5–XRN1 complex in miR-363 turnover. In addition, using recombinant IFIT5 protein with or without XRN1 enzyme, the result (Fig. 5G; Supplementary Fig. S5F) clearly indicated that both IFIT5 and XRN1 proteins are required to degrade pre-miR-363 transcript *in vitro*. Similarly, the pre-SS^{6}Mut-miR-363 is more sensitive to rIFIT5–XRN1 complex-mediated degradation than pre-DSMut-miR-363 (Fig. 5H; Supplementary Fig. S5G). Overall, these data demonstrate that the IFIT5–XRN1 complex is responsible for the degradation of pre-miR-363.

The effect of IFNγ on miR-101, miR-128, and miR-363 processing mediated by IFIT5

To survey additional miRNAs subjected to IFIT5-mediated precursor miRNA degradation, we performed miRNA microarray screening in IFIT5-overexpressing LAPC4-Con and IFIT5-siRNA KD LAPC4-KD cells (Supplementary Table S3). In particular, among IFIT5-regulated miRNA candidates, both miR-101 and miR-128 appear to have 5′-end single nucleotide overhang structure similar to the pre-miR-363 (Supplementary Table S3) and exhibit tumor suppressor function. We further confirmed that the presence of IFIT5 reduced the expression of mature miR-101 and miR-128 as well as miR-363 in PC3 cell line (Fig. 6A). In contrast, IFIT5-KD in LAPC4-KD cells increased the expression of all three miRNAs (Supplementary Fig. S6A). Also, XRN1 KD in IFIT5-expressing cells could rescue the expression levels of mature miR-363, miR-101 and miR-128 (Supplementary Fig. S6B), indicating the requirement of XRN1 in IFIT5 complex in degrading these miRNAs. Similarly, IFNγ treatment resulted in reducing the expression of miR-101, miR-128, and miR-363 (Fig. 6B). This inhibitory effect of IFNγ can be reversed or diminished by knocking down IFIT5, STAT1, or XRN1 (Fig. 6C). Similarly, overexpression of DAB2IP in PC3 cells also diminished the inhibitory effect of IFNγ on the suppression of miR-101, miR-128, and miR-363 level (Supplementary Fig. S6C), supporting the key role of IFIT5 in IFNγ-elicited precursor miRNAs processing. Based on the 3′UTR sequence, ZEB1 mRNA was predicted as a common target for both miR-101 and miR-128 (Supplementary Fig. S6D), and the results indeed indicated that both miR-101 and miR-128 could suppress ZEB1 mRNA levels (Supplementary Fig. S6D).

By comparing the precursor structures of miR-101 and miR-128, it appeared that both pre-miR-101 and pre-miR-128 have similar 5′-end structure with pre-miR-363 (Supplementary Table S3), we therefore generated two mutant constructs: one with 5′-end single stranded overhang (SSMut) and the other with double-stranded blunt end (DSMut; Fig. 6D and E) to test their expression in IFIT5-expressing PC3 and LAPC4-KD cell lines. As we expected, DSMuts were resistant to IFIT5-elicited miRNA degradation and resulted in elevated expression of mature miRNA in PC3 (Fig. 6F and G) and LAPC4-KD cells (Supplementary Fig. S6E and S6F). Again, DSMuts appeared to degrade ZEB1 more efficiently in PC3 (Fig. 6F and G) and LAPC4-KD cells (Supplementary Fig. S6E and S6F), which are correlated with the suppression of cell invasion in PC3 cells (Fig. 6H and I) and cell migration in LAPC4-KD cells (Supplementary Fig. S6E and S6F). Overall, the effect of IFIT5–XRN1 complex on pre-miR-101/128/363 processing is unique with respect to the similar 5′-end overhang structure.

Effect of IFNγ on EMT mediated by IFIT5

Based on the mechanism of action of IFIT5–XRN1 complex in the degradation of miRNAs that can target EMT factors, we further examined whether IFNγ could elicit EMT by suppressing these miRNAs via STAT1 signal axis and its downstream effector–IFIT5/XRN1 complex. Indeed, IFNγ treatment increased the PC3 cell invasion (Fig. 7A) and migration (Supplementary Fig. S7A) that was diminished in the absence of STAT1 or IFIT5 (Fig. 7A; Supplementary Fig. S7A), which is consistent with the expression of EMT factors (Slug and ZEB1) or decrease in the mesenchymal marker (vimentin) or increase in the epithelial marker (E-cadherin; Fig. 7B and C). As we expected, the expression of all these three miRNAs was inhibited by IFNγ in a dose-dependent manner (Fig. 6C) and IFNγ failed to suppress the expression of these miRNAs in the absence of XRN1, STAT1, or IFIT5 (Fig. 6C) in which no induction of Slug and ZEB1 mRNA was detected (Fig. 7D). Similarly, the effect of IFNγ on Slug and ZEB1 mRNA induction can be diminished in cells transiently transfected with miR-101, miR-128, or miR-363 (Supplementary Fig. S7B).

Apparently, IFNγ is capable of inducing EMT at low concentrations that are not antitumorigenic or antiproliferation (Supplementary Fig. S7C); its direct antitumor activity is known at much higher concentration (>1,000 ng/mL; ref. 21). These data provide new evidence that IFNγ is a potent inducer of EMT via STAT1–IFIT5/XRN1 signal axis of miRNA regulation.

The clinical correlation of IFIT5, miRNAs, and EMT biomarkers in prostate cancer

To examine the *in vivo* effect of IFNγ on prostate cancer metastasis and the role of IFIT5 in this event, we treated control and IFIT5-KD PC3 cells with IFNγ for 48 hours then cells were injected intravenously into SCID animal via tail vein. IFNγ treatment significantly increases the number and size of metastatic nodules at lung parenchyma, in contrast, loss of IFIT5 dramatically reduces metastasis of prostate cancer with or without IFNγ (Fig. 7E and F; Supplementary Table S4). Furthermore, we demonstrated the effect of IFNγ on EMT clinically, we used an *ex vivo* culture system (16) using human prostate cancer specimens and data indicated that IFNγ was able to induce the expression of IFIT5, ZEB1, Slug (Fig. 7G), and

Published OnlineFirst November 30, 2018; DOI: 10.1158/0008-5472.CAN-18-2207

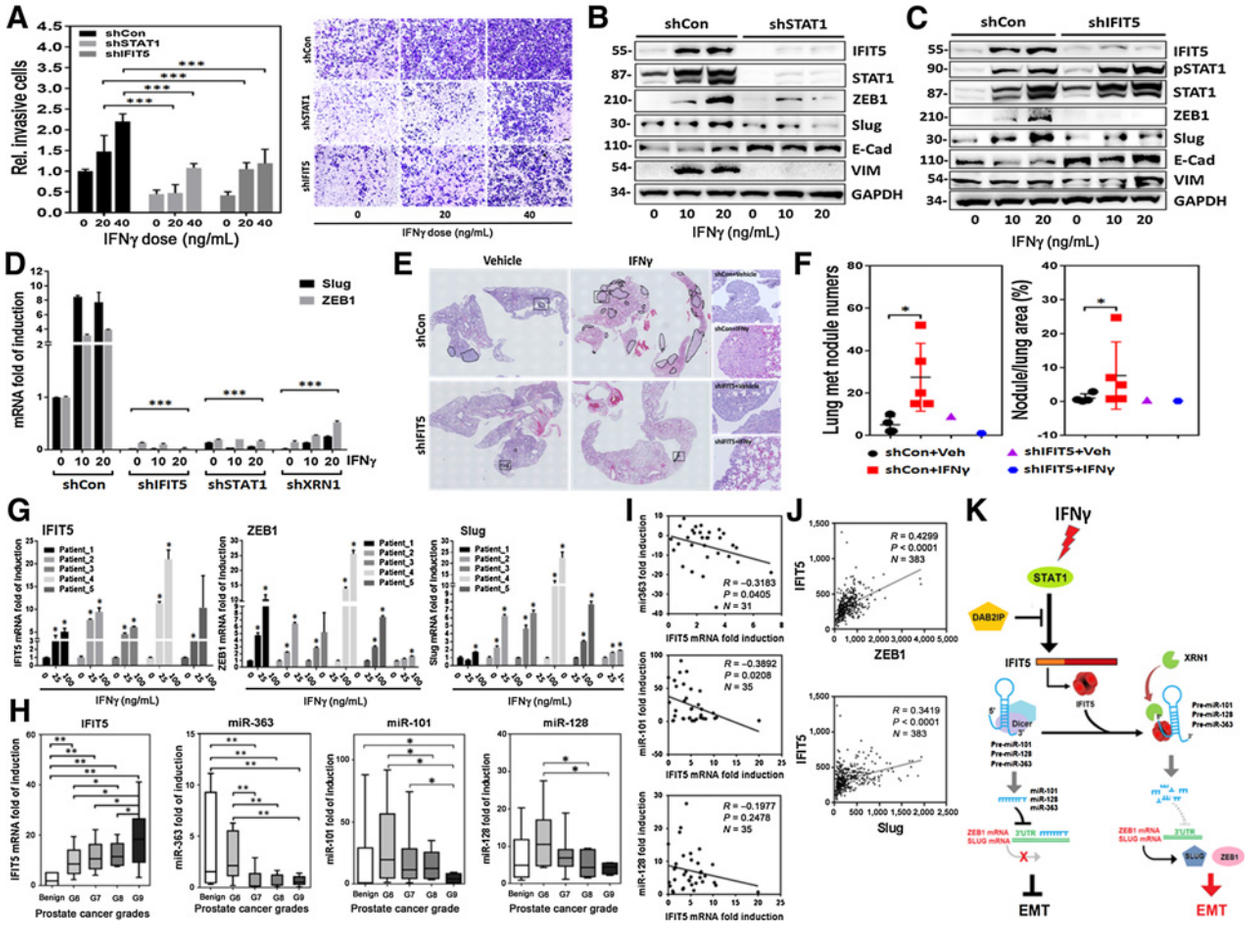

Figure 7.

IFNγ elicits its impact on EMT via activating IFIT5–XRN1-mediated miRNA turnover through STAT1 signaling pathway. **A,** Transwell invasion of STAT1- or IFIT5-KD (shSTAT1, shIFIT5) PC3 cells after treatment of IFNγ for 48 hours, compared with vector control (shCon). Invaded cells were stained with crystal violet and quantified at OD 555 nm (scale bar, 100 μm). Each bar represents mean ± SD of three replicated experiments. ***, $P < 0.0001$. **B** and **C,** Induction of IFIT5, E-cadherin, and mesenchymal factors (ZEB1, Slug, and vimentin) in STAT1- or IFIT5-KD (shSTAT1 or shIFIT5) PC3 cell lines in response to IFNγ treatment, compared with PC3 cells with control vector (shCon). **D,** IFNγ-induced expression level of Slug and ZEB1 mRNA in PC3 cells with KD of IFIT5 (shIFIT5), STAT1 (shSTAT1), or XRN1 (shXRN1), compared with vector control (shCon). ***, $P < 0.0001$. **E,** Hematoxylin and eosin staining of lung tissue derived from mice receiving tail vein intravenous injection of IFIT5-KD PC3 cells (PC3-shIFIT5) pretreated with vehicle (Veh, PBS) or IFNγ (20 ng/mL), compared with PC3 cells transfected with control vector (shCon). The black dotted line-circles region indicate the presence of metastatic nodules observed at lung parenchyma. Representative tumor nodules from each group are shown at right side panels (scale bar, 100 μm). **F,** Comparison of tumor nodule numbers and comparative area ratio in the lung parenchyma among each group. *, $P < 0.05$. **G,** Induction level of IFIT5, ZEB1, and Slug mRNA expression in *ex vivo* culture of human prostate cancer specimens treated with IFNγ for 48 hours, compared with vehicle control. *, $P < 0.05$. **H,** Relative expression level of IFIT5 mRNA and mature miR-363, miR-101, and miR-128 level in human prostate cancer specimens derived from different grades including benign ($N = 10$), G6 ($N = 9$), G7($N = 9$), G8($N = 6$), and G9($N = 7$). *, $P < 0.05$; **, $P < 0.0001$. **I,** Clinical correlation of miR-363, miR-101, and miR-128 with IFIT5 mRNA expression in human prostate cancer specimens graded from benign, G6 to G9. **J,** Clinical correlation between IFIT5 and ZEB1 or Slug mRNA level in prostate cancer from TCGA prostate cancer dataset. **K,** Schematic representing IFN-induced IFIT5-mediated precursor miRNA degradation leading to EMT in cancer. All quantitative data of mRNA or miRNA expression level were analyzed using ΔC_t (C_t value normalized to internal 18S RNA or snord95 miRNA) and $\Delta\Delta C_t$ (difference between the ΔC_t of control and experimental groups) values to obtain the fold change after normalizing with control.

vimentin (Supplementary Fig. S7D) genes whereas miR-363, miR-101, and miR-128 levels were significantly suppressed by IFNγ treatment (Supplementary Fig. S7E). Meanwhile, the level of miR-363, miR-101, and miR-128 in these *ex vivo* specimens is inversely correlated with the clinic-pathologic stage of prostate cancer patient donors (Supplementary Table S5; Supplementary Fig. S7F). We also surveyed the expression status of IFIT5 from different grades of prostate cancer specimens and data (Fig. 7H) indicate that IFIT5 mRNA levels were significantly elevated in the high-grade prostate cancer. As expected, the expression pattern of miR-363, miR-101, and miR-128 levels was opposite to that of IFIT5 (Fig. 7H), which is consistent with our observation from tissue culture cell lines. In contrast, miR-92a-2 and miR-19b-2 known as oncomirs, exhibited an elevated expression pattern in prostate cancer tissues compared with normal tissues (Supplementary Fig. S7G), supporting the specificity of IFIT5 on miRNA degradation. Meanwhile, data from prostate cancer specimens also demonstrated a similar

Published OnlineFirst November 30, 2018; DOI: 10.1158/0008-5472.CAN-18-2207

correlation between IFIT5 mRNA and miR-363 or miR-101 (Fig. 7I). In addition, analyses of EMT factors or markers in a The Cancer Genome Atlas (TCGA) prostate cancer dataset demonstrated a positive correlation between IFIT5 and ZEB1 (or Slug; Fig. 7J), and vimentin (Supplementary Fig. S7H).

Discussion

A recent study using whole exon and whole transcriptome sequencing of patients with metastatic tumors demonstrated a strong correlation between cancer metastasis and the expression of interferon-induced genes or EMT. Prostate cancer is often found to have many different kinds of infiltrated immune cells such as macrophages, dendritic cells, and tumor-infiltrating lymphocytes. Instead of eliciting tumor immunity, these immune cells with secreting cytokines are capable of facilitating prostate cancer development. For example, a study has demonstrated that fibroblast growth factor 11 (FGF11) released by the recruited $CD4^+$ T cells can induce cell invasion by increasing matrix metalloproteinase 9 (MMP9) in prostate cancer cells (22). In addition, IL4 produced from $CD4^+$ T cells has shown to increase prostate cancer cell survival and proliferation by activating the JNK signaling pathway in cancer cells (23). Moreover, IL17 secreted from T helper cells is capable of facilitating prostate cancer invasiveness by increasing several EMT transcription factors and MMP7 (24).

However, IFNγ, a type II IFN derived predominantly from $CD4^+$/$CD8^+$ lymphocytes and NK cell, is shown to have antitumor activities during innate immune response. Also, IFNγ has been used as a therapeutic agent exhibiting antiproliferative (25), antimetastatic (26), pro-apoptotic (27–30), and anti-angiogenesis (31–34) effects in various cancer types. However, several reports indicate that IFNγ could also facilitate tumor progression. For example, IFNγ can elicit $CD4^+$ T-cell loss and impair secondary antitumor immune responses after initial immunotherapy using tumor-bearing mouse model (35). In colorectal carcinoma, IFNγ has been shown to facilitate the induction of indoleamine 2,3-dioxygenase (IDO) that induces the production of kynurenines metabolites and impairs the function of surrounding T cells (36). In addition to its role in immune modulation, blockade of IFNγ receptor (IFNGR) can inhibit peritoneal disseminated tumor growth of ovarian cancer (37). Noticeably, serum IFNγ levels become elevated after radiotherapy in patients with prostate cancer (38). Nevertheless the effect of IFNγ on the overall survival of patients with prostrate cancer remains controversial (39).

In our study, we provide additional evidence that IFNγ is capable of inducing EMT, leading to cancer invasiveness via IFIT5-mediated turnover of tumor suppressor miRNAs (Fig. 6). We also noticed that low concentration of IFNγ without cytotoxicity is capable of inducing EMT of prostate cancer (Fig. 7). To strengthen the clinical evidence of IFN-induced EMT, we treated *ex vivo* prostate cancer explants with IFNγ and demonstrated that IFNγ could induce similar elevations of IFIT5 and EMT transcriptional factors and suppression of miR-101, miR-128, and miR-363 (Fig. 7G; Supplementary Fig. S7E). Taken together, these data show that IFNγ has a biphasic effect on cancer development. Nevertheless, the protumorigenic effect of IFNγ at low concentration is expected to raise a concern for its application as an antitumor or immunotherapeutic agent.

Unlike other IFIT family proteins, IFIT5 is characterized as a monomeric protein that is capable of binding to viral RNA with 5′-triphosphate group (4) and a broad spectrum of cellular RNA with either 5′-monophosphate or 5′-triphosphate group, including tRNA and other RNA polymerase III transcripts (6). However, the interaction of IFIT5 with miRNA is largely unknown. Knowing that precursor miRNA shares a similar stem loop structure with tRNA and a precursor miRNA still retains 5′-monophosphate group after processing from its primary transcript, we are able to show that IFIT5 is capable of interacting with 5′-end of pre-miRNA molecules. After binding to pre-miRNA, IFIT5 recruits XRN1 to form unique miRNA turnover complex (Fig. 5). For the first time, we demonstrated that the specificity of miRNA recognition by IFIT5 is mainly determined by the 5′-end overhang structure of pre-miRNAs (Figs. 4 and 6). Interestingly, these three tumor suppressor miRNAs (i.e., miR-101, miR-128, and miR-363) share similar 5′-end structure in their pre-miRNA and function in suppressing EMT despite of targeting different EMT transcriptional factors such as ZEB1 and Slug.

To conclude, our study provides a new functional role of IFIT5 in miRNA biogenesis (Fig. 7K), particularly, a new understanding of differential regulation of cluster miRNAs.

Until now, the clinical correlation of IFIT5 in prostate cancer is largely undetermined. In this study, we were able to demonstrate that the expression of IFIT5 is elevated in high-grade prostatic tumor and inverse correlation between IFIT5 and miR-101, -128, and -363 in prostate cancer tumor specimens as well as from prostate cancer TCGA database; this correlative relationship was not observed in other members of the miR-106a-363 cluster. In addition, a significant clinical correlation between IFIT5 and EMT transcription factors (ZEB1 or Slug) was observed from prostate cancer TCGA dataset, which supports the regulatory network of IFIT5-miRNAs-EMT in prostate cancer. Also, data from explants provide additional evidence for the promoting effect of IFNγ on prostate cancer progression, Taking together, we have unveiled new function of IFNγ related with prostate cancer progression and potential therapeutic target(s) from its underlying mechanism.

Disclosure of Potential Conflicts of Interest

G.V. Raj reports receiving other commercial research support from Bayer, has received speakers bureau honoraria from Astellas and Pfizer, and has ownership interest (including stock, patents, etc.) in EtiraRx, GaudiumRx, and C-diagnostics. No potential conflicts of interest were disclosed by the other authors.

Authors' Contributions

Conception and design: U-G. Lo, G.V. Raj

Development of methodology: U-G. Lo, D. Yang, C.-J. Lin, R. Sonavane, P. Kapur, G.V. Raj

Acquisition of data (provided animals, acquired and managed patients, provided facilities, etc.): L. Gandee, E. Hernandez, J. Santoyo, S. Ma, R. Sonavane, J. Huang, P. Kapur, G.V. Raj, C.-H. Lai

Analysis and interpretation of data (e.g., statistical analysis, biostatistics, computational analysis): U-G. Lo, J. Santoyo, L. Moro, A.A. Arbini, P. Kapur, G.V. Raj

Writing, review, and/or revision of the manuscript: U-G. Lo, A.A. Arbini, G.V. Raj, D. He, J.-T. Hsieh

Administrative, technical, or material support (i.e., reporting or organizing data, constructing databases): R.-C. Pong, L. Gandee, A. Dang, J. Santoyo, S.-F. Tseng, H. Lin

Study supervision: J.-T. Hsieh

Acknowledgments

We thank Dr. Collins (University of California, Berkeley, CA) for providing IFIT5 cDNA constructs, Dr. Dong (Emory University, Atlanta, GA) for providing the psiCHECK2-Slug3′UTR plasmid. Drs. Kou-Juey Wu (China Medical University, Taichung, Taiwan) and Dr. Vimal Selvaraj (Cornell University, Ithaca, NY) for the helpful discussion. We also acknowledge the assistance of the Southwestern Small Animal Imaging Resource, which is supported in part by the Harold C. Simmons Cancer Center through an NCI Cancer Center Support Grant (1P30 CA142543), and the Department of Radiology (NIH 1S10RR024757). This work was supported by grants from the United States Army (W81XWH-11-1-0491 and W81XWH-16-1-0474 to J.-T. Hsieh) and (W81XWH-14-1-0249 to U.-G. Lo), and the Ministry of Science and Technology in Taiwan (MOST103-2911-I-005-507 to H. Lin).

The costs of publication of this article were defrayed in part by the payment of page charges. This article must therefore be hereby marked *advertisement* in accordance with 18 U.S.C. Section 1734 solely to indicate this fact.

Received July 18, 2018; revised October 23, 2018; accepted November 27, 2018; published first November 30, 2018.

References

1. Hildenbrand B, Sauer B, Kalis O, Stoll C, Freudenberg MA, Niedermann G, et al. Immunotherapy of patients with hormone-refractory prostate carcinoma pre-treated with interferon-gamma and vaccinated with autologous PSA-peptide loaded dendritic cells—a pilot study. Prostate 2007;67:500–8.
2. Street SE, Cretney E, Smyth MJ. Perforin and interferon-gamma activities independently control tumor initiation, growth, and metastasis. Blood 2001;97:192–7.
3. de Veer MJ, Holko M, Frevel M, Walker E, Der S, Paranjape JM, et al. Functional classification of interferon-stimulated genes identified using microarrays. J Leukoc Biol 2001;69:912–20.
4. Abbas YM, Pichlmair A, Gorna MW, Superti-Furga G, Nagar B. Structural basis for viral 5′-PPP-RNA recognition by human IFIT proteins. Nature 2013;494:60–4.
5. Katibah GE, Lee HJ, Huizar JP, Vogan JM, Alber T, Collins K. tRNA binding, structure, and localization of the human interferon-induced protein IFIT5. Mol Cell 2013;49:743–50.
6. Katibah GE, Qin Y, Sidote DJ, Yao J, Lambowitz AM, Collins K. Broad and adaptable RNA structure recognition by the human interferon-induced tetratricopeptide repeat protein IFIT5. Proc Natl Acad Sci U S A 2014;111:12025–30.
7. Aalto AP, Pasquinelli AE. Small non-coding RNAs mount a silent revolution in gene expression. Curr Opin Cell Biol 2012;24:333–40.
8. Schickel R, Boyerinas B, Park SM, Peter ME. MicroRNAs: key players in the immune system, differentiation, tumorigenesis and cell death. Oncogene 2008;27:5959–74.
9. Obernosterer G, Leuschner PJ, Alenius M, Martinez J. Post-transcriptional regulation of microRNA expression. RNA 2006;12:1161–7.
10. Dylla L, Jedlicka P. Growth-promoting role of the miR-106a∼363 cluster in Ewing sarcoma. PLoS One 2013;8:e63032.
11. Chow TF, Mankaruos M, Scorilas A, Youssef Y, Girgis A, Mossad S, et al. The miR-17-92 cluster is over expressed in and has an oncogenic effect on renal cell carcinoma. J Urol 2010;183:743–51.
12. Diosdado B, van de Wiel MA, Terhaar Sive Droste JS, Mongera S, Postma C, Meijerink WJ, et al. MiR-17-92 cluster is associated with 13q gain and c-myc expression during colorectal adenoma to adenocarcinoma progression. Br J Cancer 2009;101:707–14.
13. Wong P, Iwasaki M, Somervaille TC, Ficara F, Carico C, Arnold C, et al. The miR-17-92 microRNA polycistron regulates MLL leukemia stem cell potential by modulating p21 expression. Cancer Res 2010;70:3833–42.
14. Landais S, Landry S, Legault P, Rassart E. Oncogenic potential of the miR-106–363 cluster and its implication in human T-cell leukemia. Cancer Res 2007;67:5699–707.
15. Xie D, Gore C, Liu J, Pong RC, Mason R, Hao G, et al. Role of DAB2IP in modulating epithelial-to-mesenchymal transition and prostate cancer metastasis. Proc Natl Acad Sci U S A 2010;107:2485–90.
16. Ravindranathan P, Lee TK, Yang L, Centenera MM, Butler L, Tilley WD, et al. Peptidomimetic targeting of critical androgen receptor-coregulator interactions in prostate cancer. Nat Commun 2013;4:1923.
17. Min J, Zaslavsky A, Fedele G, McLaughlin SK, Reczek EE, De Raedt T, et al. An oncogene-tumor suppressor cascade drives metastatic prostate cancer by coordinately activating Ras and nuclear factor-kappaB. Nat Med 2010;16:286–94.
18. Jones CI, Zabolotskaya MV, Newbury SF. The 5′ → 3′ exoribonuclease XRN1/Pacman and its functions in cellular processes and development. Wiley Interdiscip Rev RNA 2012;3:455–68.
19. Nagarajan VK, Jones CI, Newbury SF, Green PJ. XRN 5′→3′ exoribonucleases: structure, mechanisms and functions. Biochim Biophys Acta 2013;1829:590–603.
20. Jones CI, Grima DP, Waldron JA, Jones S, Parker HN, Newbury SF. The 5′-3′ exoribonuclease Pacman (Xrn1) regulates expression of the heat shock protein Hsp67Bc and the microRNA miR-277-3p in Drosophila wing imaginal discs. RNA Biol 2013;10:1345–55.
21. Wall L, Burke F, Barton C, Smyth J, Balkwill F. IFN-gamma induces apoptosis in ovarian cancer cells in vivo and in vitro. Clin Cancer Res 2003;9:2487–96.
22. Hu S, Li L, Yeh S, Cui Y, Li X, Chang HC, et al. Infiltrating T cells promote prostate cancer metastasis via modulation of FGF11→miRNA-541→androgen receptor (AR)→MMP9 signaling. Mol Oncol 2015;9:44–57.
23. Roca H, Craig MJ, Ying C, Varsos ZS, Czarnieski P, Alva AS, et al. IL-4 induces proliferation in prostate cancer PC3 cells under nutrient-depletion stress through the activation of the JNK-pathway and survivin up-regulation. J Cell Biochem 2012;113:1569–80.
24. Zhang Q, Liu S, Parajuli KR, Zhang W, Zhang K, Mo Z, et al. Interleukin-17 promotes prostate cancer via MMP7-induced epithelial-to-mesenchymal transition. Oncogene 2017;36:687–99.
25. Aune TM, Pogue SL. Inhibition of tumor cell growth by interferon-gamma is mediated by two distinct mechanisms dependent upon oxygen tension: induction of tryptophan degradation and depletion of intracellular nicotinamide adenine dinucleotide. J Clin Invest 1989;84:863–75.
26. Addison CL, Arenberg DA, Morris SB, Xue YY, Burdick MD, Mulligan MS, et al. The CXC chemokine, monokine induced by interferon-gamma, inhibits non-small cell lung carcinoma tumor growth and metastasis. Hum Gene Ther 2000;11:247–61.
27. Fukui T, Matsui K, Kato H, Takao H, Sugiyama Y, Kunieda K, et al. Significance of apoptosis induced by tumor necrosis factor-alpha and/or interferon-gamma against human gastric cancer cell lines and the role of the p53 gene. Surg Today 2003;33:847–53.
28. Burke F, East N, Upton C, Patel K, Balkwill FR. Interferon gamma induces cell cycle arrest and apoptosis in a model of ovarian cancer: enhancement of effect by batimastat. Eur J Cancer 1997;33:1114–21.
29. Suk K, Chang I, Kim YH, Kim S, Kim JY, Kim H, et al. Interferon gamma (IFNgamma) and tumor necrosis factor alpha synergism in ME-180 cervical cancer cell apoptosis and necrosis. IFNgamma inhibits cytoprotective NF-kappa B through STAT1/IRF-1 pathways. J Biol Chem 2001;276:13153–9.
30. Chung TW, Tan K-T, Chan H-L, Lai M-D, Yen M-C, Li Y-R, et al. Induction of indoleamine 2,3-dioxygenase (IDO) enzymatic activity contributes to interferon-gamma induced apoptosis and death receptor 5 expression in human non-small cell lung cancer cells. Asian Pac J Cancer Prev 2014;15:7995–8001.
31. Ribatti D, Nico B, Pezzolo A, Vacca A, Meazza R, Cinti R, et al. Angiogenesis in a human neuroblastoma xenograft model: mechanisms and inhibition by tumour-derived interferon-gamma. Br J Cancer 2006;94:1845–52.
32. Saiki I, Sato K, Yoo YC, Murata J, Yoneda J, Kiso M, et al. Inhibition of tumor-induced angiogenesis by the administration of recombinant interferon-gamma followed by a synthetic lipid-A subunit analogue (GLA-60). Int J Cancer 1992;51:641–5.
33. Strieter RM, Kunkel SL, Arenberg DA, Burdick MD, Polverini PJ. Interferon gamma-inducible protein 10 (IP-10), a member of the C-X-C chemokine

Published OnlineFirst November 30, 2018; DOI: 10.1158/0008-5472.CAN-18-2207

family, is an inhibitor of angiogenesis. Biochem Biophys Res Commun 1995;210:51–7.
34. Sun T, Yang Y, Luo X, Cheng Y, Zhang M, Wang K, et al. Inhibition of tumor angiogenesis by interferon-gamma by suppression of tumor-associated macrophage differentiation. Oncol Res 2014;21:227–35.
35. Berner V, Liu H, Zhou Q, Alderson KL, Sun K, Weiss JM, et al. IFN-gamma mediates CD4+ T-cell loss and impairs secondary antitumor responses after successful initial immunotherapy. Nat Med 2007;13:354–60.
36. Mellor AL, Munn DH. Tryptophan catabolism prevents maternal T cells from activating lethal anti-fetal immune responses. J Reprod Immunol 2001;52:5–13.
37. Abiko K, Matsumura N, Hamanishi J, Horikawa N, Murakami R, Yamaguchi K, et al. IFN-gamma from lymphocytes induces PD-L1 expression and promotes progression of ovarian cancer. Br J Cancer 2015;112:1501–9.
38. Tanji N, Kikugawa T, Ochi T, Taguchi S, Sato H, Sato T, et al. Circulating cytokine levels in patients with prostate cancer: effects of neoadjuvant hormonal therapy and external-beam radiotherapy. Anticancer Res 2015;35:3379–83.
39. Hastie C, Masters JR, Moss SE, Naaby-Hansen S. Interferon-gamma reduces cell surface expression of annexin 2 and suppresses the invasive capacity of prostate cancer cells. J Biol Chem 2008;283:12595–603.

Cancer Research
The Journal of Cancer Research (1916–1930) | The American Journal of Cancer (1931–1940)

AACR American Association for Cancer Research

IFNγ-Induced IFIT5 Promotes Epithelial-to-Mesenchymal Transition in Prostate Cancer via miRNA Processing

U-Ging Lo, Rey-Chen Pong, Diane Yang, et al.

Cancer Res 2019;79:1098-1112. Published OnlineFirst November 30, 2018.

Cancer Research

IFNγ, a Double-Edged Sword in Cancer Immunity and Metastasis

Chengfei Liu and Allen C. Gao

IFNγ has antitumorigenic effects; however, the findings of IFNγ in promoting the tumor cell survival and inducing adaptive immune resistance via $CD4^+$ T-cell loss and programmed death ligand 1 (PD-L1) upregulation challenge this concept. Lo and colleagues determined that IFNγ induces epithelial–mesenchymal transition (EMT) by regulating the turnover of miRNA in prostate cancer, emphasizing the duplicitous effects of IFNγ. IFIT5, an IFN-induced tetratricopeptide repeat (IFIT) family member, was found to form a complex with the exoribonuclease-XRN1 to process miRNA maturation. These findings unveil a new IFNγ–STAT1–IFIT5–miRNA–EMT pathway in prostate cancer progression. The biphasic effects of IFNγ in prostate cancer raise concerns about its therapeutic application, which need to be evaluated in future studies.

See related article by Lo et al., p. 1098

In this issue of *Cancer Research*, Lo and colleagues (1) describe an interesting observation wherein IFNγ induces epithelial–mesenchymal transition (EMT) in prostate cancer cells by regulating the degradation of precursor miRNAs through a complex between the known IFNγ-stimulated RNA-binding protein, interferon-induced tetratricopeptide 5 (IFIT5), and the exoribonuclease candidate XRN1 (IFIT5-XRN1). Their study emerged from research on the GTPase-activating protein, DAB2IP, which has long been a focus for this group. They found that IFNγ promotes EMT in prostate cancer cells through DAB2IP, which has been previously identified as an upstream regulator of EMT, and went on to profile the miRNAs and show that miR-363 expression and maturation are specifically regulated by DAB2IP and that IFIT5 is a key factor regulating miR-363 turnover. The authors next sought to further characterize the network among IFIT5, miRNA, and EMT in prostate cancer. They first discovered that miR-363 suppresses EMT by targeting Slug in prostate cancer cells and that IFIT5 recognizes the unique 5′-end overhanging structure of pre-miR-363 to target it for degradation. Because IFIT5 does not possess ribonuclease activity, the authors then demonstrated that IFIT5 alone is not sufficient in regulating miRNA maturation and degradation but needs to form a complex with exoribonuclease-XRN1 to promote miR-363 turnover. To expand the overall effects of the network they established, the authors further examined other miRNAs that could be regulated by IFNγ. Two additional miRNAs, miR-101 and miR-128, were also identified to be involved in the IFIT5-EMT process. Finally, they found that IFIT5 is inversely correlated with miR-363, miR-101, and miR-128 and positively correlated with EMT markers ZEB1, Slug, and vimentin in prostate cancer specimens. From benchwork to clinical validation, Lo and colleagues identified a network of immune factors, transcriptional factors, and miRNAs involved in prostate cancer progression and metastasis.

Although we now recognize that miRNA plays crucial roles in prostate cancer progression, regulation of miRNA expression remains largely unknown. After transcription, pre-miRNA undergoes nuclear and cytoplasmic processing to become mature miRNA. Alteration of mature miRNA expression occurs in many different ways, such as SNP, miRNA tailing, editing, methylation, and regulation of stability (2). XRN1 is a 5′-3′ exoribonuclease that predominantly degrades miRNAs after they have been decapped in cells. Lo and colleagues discovered for the first time that IFIT5 recruits XRN1 to form a unique miRNA complex with the 5′-end of pre-miRNA molecules. The reciprocal correlation of IFIT5 and miR-363 and miR-101 expression in prostate cancer specimens further supports the role of IFNγ signaling in miRNA regulation. Human IFNγ is predominantly from infiltrating immune cells and whether this correlation also exists in these cells in prostate tumors needs to be investigated in future studies. Nevertheless, this function of IFIT5 in miRNA processing provides a new piece of evidence that IFNγ signaling regulates miRNA maturation and turnover in prostate cancer.

Over the last few decades, our understanding of the role of IFNγ in cancer immunity has been evolving. Numerous studies have reported that IFNγ is an important cytokine that facilitates both the innate and adaptive immune systems. Initial induction of IFNγ significantly suppresses tumor growth via immune activation; however, it can also induce $CD4^+$ T-cell apoptosis, alter the CD4:CD8 ratio, and subsequently impair secondary antitumor immune responses (3). As a type II IFN, IFNγ plays both pro- and antitumorigenic roles in immunoediting, a process that consists of immunosurveillance and tumor progression (4). IFNγ plays a role in all three phases of the immunoediting process: elimination, equilibrium, and escape. During the elimination phase, natural killer (NK) cells, NK T cells, $CD8^+$, and $CD4^+$ T cells secrete IFNγ, which then activates macrophages, dendritic cells, Th1 $CD4^+$ helper T cells, and B cells that lead to complete tumor elimination, suggesting that IFNγ is predominantly antitumorigenic in the tumor environment during this phase. During the equilibrium phase, the immune system is able to maintain

Department of Urology, Comprehensive Cancer Center, University of California Davis, Sacramento, California.

Corresponding Author: Allen C. Gao, Department of Urology, School of Medicine, University of California, Davis, Research III Bldg, Suite 1300, 4645 2nd Ave, Sacramento, CA 95817. Phone: 916-734-8718; Fax: 916-734-8714; E-mail: acgao@ucdavis.edu

doi: 10.1158/0008-5472.CAN-19-0083

immune-mediated tumor dormancy. This phase is poorly understood, in part, because of technical challenges in establishing mouse models, but it is known that IFNγ is required for maintaining tumor dormancy by inducing cancer senescence. Finally, during the escape phase, tumor cells grow and expand through mechanisms including adaptive and acquired immune resistance (5). Recent studies suggest that IFNγ can upregulate the expression of programmed-death ligand 1 (PD-L1), a membrane-bound immune inhibitory molecule on the surface of tumor cells. Because PD-L1 binds to programmed cell death protein 1 (PD1) expressed on the activated $CD8^+$ T cells and leads to apoptotic T-cell death, IFNγ signaling activation facilities tumor cells escaping from the antitumor $CD8^+$ T-cell cytotoxicity through formation of the immunosuppressive tumor microenvironment, promotes tumor cell survival, and induces adaptive resistance (6). Therefore, IFNγ possibly plays a protumorigenic role during the tumor immunity escape stage. Although application of immunotherapy in prostate cancer lags behind that in other cancer types, several clinical trials testing immune checkpoint inhibitors in patients with prostate cancer have begun (7). The exact role of IFNγ in prostate cancer immunity remains to be determined and the study by Lo and colleagues brings up more concern into the prostate cancer immunotherapy arena by reinforcing the dual nature of IFNγ in prostate cancer progression.

Metastasis is the primary underlying cause of fatality in patients with prostate cancer. Bone metastases occur in more than 90% of patients with advanced prostate cancer and are associated with poor survival. For men with metastatic prostate cancer, only one-third survive for 5 years after diagnosis (8). There is an urgent need to unravel potential resistant mechanisms that perpetuate disease progression during effective androgen receptor blockade and to devise ways of targeting resistant pathways. EMT is believed to be a crucial step in the conversion of early-stage disease to invasive and metastatic cancer (9). Immortalized human mammary epithelial cells acquire the mesenchymal phenotype and express stem cell markers after induction of EMT (10). The aberrant expression and localization of E-cadherin, N-cadherin, vimentin, Wnt5A, and ZEB1 appears to be important in prostate cancer invasion and bone metastasis. Although strong evidence supports EMT as the essential step in the progression and metastasis of prostate cancer, difficulties in identifying migratory cancer cells have precluded confirmation of the occurrence of EMT *in vivo* for many years. Thus, better understanding of upstream EMT regulators is urgent and important in the clinical arena. EMT can be triggered by tumor-associated fibroblasts, immune cells, and secreted soluble factors, such as Wnt ligands, TGFβ, EGF, and hepatocyte growth factor. These factors and inflammatory cytokines can exert their effects through autocrine or paracrine systems. Slug, Snail, ZEB1, ZEB2, and Twist have been previously identified as classical EMT regulators. In their study, Lo and colleagues report that IFNγ induces EMT in prostate cancer cells by regulating expression of EMT regulators and markers such as ZEB1, Slug, and vimentin as well as miR-363, miR-101, and miR-128. The take-home message from this comprehensive study is that the administration of IFNγ might not benefit patients with prostate cancer and possibly cause some harmful side effects. Nevertheless, clinical evidence and clinical trials would be required before this could be considered as a conclusion.

Together, IFNγ signaling is still largely unfathomable in prostate cancer. Considering the classical role of IFNγ in cancer immunoediting, the possibility of its utility in prostate cancer immunetherapy arena should not be disregarded. Prostate cancer immunotherapy awaits rigorous investigation to define the real targets and pathways involved in the therapy. A better grasp of the detailed mechanisms that underlie the effects of IFNγ in prostate cancer immunoediting appears to be necessary. Lo and colleagues have identified a novel tumor-promoting IFNγ–STAT1–IFIT5–miRNA–EMT pathway in prostate cancer cells, suggesting that IFNγ might serve as a master regulator in controlling several downstream signaling pathways, such as JAK-STAT1, IFIT5, DAB2IP, and miRNA signaling leading to prostate cancer progression and metastasis through EMT, raising concerns about its clinical application.

Disclosure of Potential Conflicts of Interest

No potential conflicts of interest were disclosed.

Acknowledgments

This commentary did not receive any specific grant from any funding agency in the public, commercial, or not-for-profit sector.

Received January 18, 2019; accepted January 18, 2019; published first March 15, 2019.

References

1. Lo UG, Pong RC, Yang D, Gandee L, Hernandez E, Dang A, et al. IFN-γ-induced IFIT5 promotes epithelial-to-mesenchymal transition in prostate cancer via miRNA processing. Cancer Res 2019;79:1098–112.
2. Ha M, Kim VN. Regulation of microRNA biogenesis. Nat Rev Mol Cell Biol 2014;15:509–24.
3. Berner V, Liu H, Zhou Q, Alderson KL, Sun K, Weiss JM, et al. IFN-gamma mediates CD4+ T-cell loss and impairs secondary antitumor responses after successful initial immunotherapy. Nat Med 2007;13:354–60.
4. Kaplan DH, Shankaran V, Dighe AS, Stockert E, Aguet M, Old LJ, et al. Demonstration of an interferon gamma-dependent tumor surveillance system in immunocompetent mice. Proc Natl Acad Sci U S A 1998;95:7556–61.
5. Alspach E, Lussier DM, Schreiber RD. Interferon gamma and its important roles in promoting and inhibiting spontaneous and therapeutic cancer immunity. Cold Spring Harb Perspect Biol 2018 April 16 [Epub ahead of print].
6. Mandai M, Hamanishi J, Abiko K, Matsumura N, Baba T, Konishi I. Dual faces of IFNgamma in cancer progression: a role of PD-L1 induction in the determination of pro- and antitumor immunity. Clin Cancer Res 2016;22:2329–34.
7. Rescigno P, de Bono JS. Immunotherapy for lethal prostate cancer. Nat Rev Urol 2019;16:69–70.
8. Gundem G, Van Loo P, Kremeyer B, Alexandrov LB, Tubio JMC, Papaemmanuil E, et al. The evolutionary history of lethal metastatic prostate cancer. Nature 2015;520:353–7.
9. Thiery JP. Epithelial-mesenchymal transitions in tumour progression. Nat Rev Cancer 2002;2:442–54.
10. Mani SA, Guo W, Liao MJ, Eaton EN, Ayyanan A, Zhou AY, et al. The epithelial-mesenchymal transition generates cells with properties of stem cells. Cell 2008;133:704–15.

IFNγ, a Double-Edged Sword in Cancer Immunity and Metastasis

Chengfei Liu and Allen C. Gao

Cancer Res 2019;79:1032-1033.